

American Rocket Society
500 Fifth Avenue
New York 36, N.Y.

AN EXPERIMENTAL INVESTIGATION OF UNSTABLE COMBUSTION
IN SOLID PROPELLANT ROCKET MOTORS

by

W. Grant Brownlee and Frank E. Marble

Presented at the ARS Solid
Propellant Rocket Research
Symposium, Princeton University,
Princeton, New Jersey,
January 28-29, 1960

Publishing rights reserved by the
American Rocket Society. Abstracts
may be published without permission
if credit is given to the author
and to ARS

AN EXPERIMENTAL INVESTIGATION OF UNSTABLE COMBUSTION
IN SOLID PROPELLANT ROCKET MOTORS^{1,2}

by

W. Grant Brownlee³ and Frank E. Marble⁴

ABSTRACT

Unstable combustion in solid propellant rocket motors is characterized by high frequency chamber pressure oscillations, often accompanied by changes in the mean burning rate. Experiments with case-bonded, cylindrically perforated motors using a polysulfide, ammonium-perchlorate propellant were reproducible as a result of careful manufacturing control and extended propellant curing time. In these motors the oscillations were in the fundamental pseudo-standing tangential mode and were accompanied by increases in the average burning rate. At sufficiently high pressure levels all firings were stable. Reduction of the operating level led to mild instability. A sufficient further reduction produced a sudden change to maximum instability. Continued reduction in pressure level from this point resulted in a gradual decrease in the degree of instability but it could not be experimentally verified that a low pressure stable region existed. The levels at which these events took place were frequency dependent and generally increased as the tangential frequency was reduced. At a given operating level, the instability became less severe when the grain length was reduced below a critical value. Increasing the length above the critical value did not affect the level at which the motors became stable. The pressure levels for stability and for maximum instability moved to lower values with decreases in the

1. This paper is based on a thesis of the same title submitted by Capt. Brownlee to the Graduate School of the California Institute of Technology in partial fulfillment of the requirements for the degree of Doctor of Philosophy, June 1959.
2. The experiments were conducted at the Jet Propulsion Laboratory, Pasadena, California under ORDCIT Project Contract No. DA-04-495 ORD 18, Department of the Army, Ordnance Corps. The authors wish to express their gratitude to all those connected with the program and in particular to Mr. G. Robillard, Chief of the Solid Propellants Rocket Section, and Dr. E.M. Landsbaum, Research Engineer, for the complete cooperation and constant encouragement so generously extended.
3. Captain, Royal Canadian Artillery, Technical Staff Officer, Grade 3, Canadian Armament Design and Engineering Establishment, Valcartier, P.Q. Mem. ARS.
4. Professor of Jet Propulsion and Mechanical Engineering, California Institute of Technology, Pasadena, California. Mem. ARS.

propellant grain temperature in a manner not entirely accounted for by the effect of grain temperature on burning rate. Stable, mildly unstable and severely unstable operation was observed throughout the range -80°F to 180°F . The maximum instability decreased with grain temperature.

Slab motors with opposed-plane grain surfaces exhibited oscillations in the transverse sloshing mode but no accompanying changes in the burning rate. Tangential oscillation of equivalent amplitude strongly affected the burning rate in the cylindric motors; hence it appears that increases in the burning rate are associated with tangential velocities rather than pressure fluctuations.

INTRODUCTION

Although the occurrence of high frequency oscillations in solid propellants rockets and the attendant deviations of mean chamber pressure have been recognized for nearly twenty years^(1,2,3) the basic facts underlying these phenomena are at best understood very poorly. This state of affairs may be taken as a measure of the inherent experimental and theoretical difficulties of the problem. Theoretical investigations^(4,5,6,7,8) are often severely hampered by lack of knowledge concerning key physical phenomena. On the other hand, experimental investigations^(9,10,11,12) present their own peculiar brand of difficulties, perhaps the most intractable of which has been to obtain reproducible results.

The preponderant portion of experimental work has been performed as an accessory to the development of military or commercial rocket motors. Naturally, the immediate practical aim has been to eliminate the instability. Consequently, it has not usually been possible to investigate the effect of varying a comprehensive group of significant parameters over broad ranges. Hence while such firings have been very informative individually, they do not collectively present an organized, complete framework of knowledge.

At present there appear to be two possible approaches to advance the understanding of unstable combustion. The first, of course, is an attack on the basis mechanism of combustion in the quasi-steady and thence, unsteady state. This lengthy pursuit has the strong advantage that in the course of the work, the majority of solid propellant combustion problems will be solved. The second approach and the one attempted in the present work, rests upon the hope that by study of carefully controlled rocket experiments entailing systematic variation of the significant parameters, one can arrive at some gross conditions governing the unstable process that rest only on facts that can be obtained from stable combustion processes and not upon detailed understanding of the propellant burning mechanism. This approach was taken successfully in connection with the high frequency oscillations in air-breathing combustion chambers. Here it was found⁽¹³⁾ that the detailed combustion information required could be obtained simply from an elementary experiment with a stable combustion chamber and hence the unsolved problems of hydrocarbon combustion kinetics and combustion in turbulent mixing zones were, to a large extent, by-passed. The present work has not yet yielded similar success with unstable burning in solid propellant rockets. The progress, however, has been most encouraging.

It was recognized at the outset that without essentially complete reproducibility of results as to when and in what manner instability occurred, the outcome of the present experiments would be largely meaningless. Consequently the first objective of this extensive series of experiments was to achieve reproducibility, and modification of quality control and curing procedures was studied accordingly. Upon achieving this aim it was possible to investigate the occurrence or non-occurrence of instability in case-bonded, cylindrically perforated motors over wide and systematic variations of propellant grain geometry, rocket chamber pressure level, grain temperature, etc. In all, some 400 rocket firings were made under highly controlled conditions. A composite propellant was used with a polysulfide fuel and ammonium perchlorate oxidizer. Some further experiments with a slab type motor elucidated certain features of combustion instability. Although the results have not as yet led to a simple picture of unstable combustion oscillations they have illuminated some features hitherto clouded through incomplete and sometimes disjointed information.

CHARACTERISTIC FEATURES OF THE UNSTABLE FIRINGS

Almost all of the motors were case-bonded and cylindrically perforated with restricted ends, as illustrated schematically in Figure 1. Certain characteristic features of the unstable operation of this type of motor will be illustrated by reference to typical firings. In Figure 2 the mean pressure (\bar{P}_c) versus time curve is shown for a cylindrical motor with nominal initial 3.0 in. perforation, 5 in. ID case, grain length of 38 in. and case length 38.5 in. For brevity this will be designated a 3 x 5 x 38/38.5 in. motor. The motor was fired at a grain temperature of 160°F with a nozzle throat diameter of 1.70 in. It is clear from the pressure-time curve that this motor was severely unstable. It may be seen that after ignition, a stable period follows. At 0.38 sec after ignition, high frequency instrumentation indicated that a gaseous oscillation was present within the grain perforation. This oscillation became observable at a level of approximately one psi peak to peak; the mean chamber pressure was 380 psia at the time. As time passed, the oscillation amplitude grew larger and the mean pressure increased correspondingly. As the oscillation became very large, a severe increase in mean pressure occurred. The mean pressure rose smoothly to 900 psia where an abrupt change in slope occurred in the \bar{P}_c vs t trace. This point will be designated the "break" in the mean pressure trace. After the break, \bar{P}_c rose more slowly with time to 1050 psia. At this point (point C), the oscillations decayed rapidly and \bar{P}_c dropped to 470 psia (point D). A second growth in instability then occurred with a maximum amplitude at point E. This terminated at point F. Finally, a period of weak instability occurred just before and during tail-off (burnout). The correlation between oscillation amplitude and mean pressure increase may be clearly seen in Figure 3. The lower two traces labelled \bar{P}_{c_h} and \bar{P}_{c_n} are mean pressure traces, measured at the head and nozzle ends of the motor, respectively. The upper three traces labelled P_{ac} , 1, 2, and 3 are indicative of the peak to peak oscillation amplitude at the head end of the cavity. Increasing oscillation amplitude is indicated by a downward deflection of these traces. It is clear that the changes in amplitude of the oscillations correlate exactly with the mean pressure deviations. The general behaviour of the motor is characteristic of all the unstable firings of cylindrically perforated motors. In every case a stable period followed ignition after which

a growth in oscillation amplitude occurred to varying degrees, depending on factors to be discussed shortly.

Mode Identification

The fundamental mode of gaseous oscillation was identified as being tangential in nature. Since the magnitude of the pressure fluctuations was finite, the linearizations of acoustic theory would be expected to be a poor approximation. However, the fundamental frequency was found to be in close agreement with that of the acoustic tangential mode even under the most severe oscillatory conditions. In order to determine this, the outputs of Photocon types 345 and 355 pressure transducers were recorded using a Jet Propulsion Laboratory modified Ampex Model 306-7, 7 channel tape recorder. The recordings were then analyzed by means of a J.P.L. developed heterodyne frequency analyzer⁽¹⁴⁾ which analyzed the complex waveforms into Fourier components as functions of time. In Figure 4 the results for the fundamental component are shown for a typical firing. The firing began at a perforation diameter of approximately 3.05 in. As the firing proceeded, the perforation diameter increased due to the consumption of propellant. The earliest detectable oscillation began with a frequency of 6.7 kc. The frequency then decreased smoothly with time as the perforation diameter increased. The oscillation diminished below a detectable level at 5.3 kc, reappeared at 4.6 kc and persisted through a portion of tail-off. Mean pressure data reduction provided a calculated value of perforation radius as a function of time. In Figure 4 it may be seen that the instantaneous product of frequency and radius is essentially constant with an average value of 10,875 in./sec. Using this value and the acoustic solutions for wave modes in a cylindrical chamber, a set of discrete possible velocities of sound may be arrived at. However, the velocity of sound may also be obtained from the relation

$$a_c = \Gamma^o c^*$$

$$\text{where} \quad \Gamma^o = \bar{\gamma} \left(\frac{2}{\bar{\gamma} + 1} \right)^{\frac{\bar{\gamma} + 1}{2(\bar{\gamma} - 1)}}$$

$\bar{\gamma}$ is an average ratio of specific heats and

c^* is the propellant characteristic exhaust velocity.

In order to obtain compatible velocities and at the same time a reasonable value of $\bar{\gamma}$ it was necessary to choose the fundamental tangential mode. This led to $\bar{\gamma} = 1.24$.

The higher frequency components of the complex waveform occurred as integral multiples of the fundamental frequency within approximately one per cent. All multiples were present, at least to 30 kc, which is twice the upper limit of the frequency analyzer. The amplitudes of the overtones were generally lower than that of the fundamental. A more precise statement cannot presently be made due to uncertainties in absolute amplitude calibration at these frequency levels.

It should be noted that the above results are in close agreement with the theoretical investigations of Maslen and Moore⁽¹⁵⁾ regarding strong transverse waves in a circular cylinder. Their results indicate that finite transverse waves can exist without the formation of shock waves. These waves consist of a fundamental component and harmonically related overtones. The frequencies are only weakly amplitude dependent. In the case of the finite wave associated with the fundamental tangential acoustic mode the lowest frequency component differs in frequency from the acoustic value by less than two per cent for a peak-to-peak pressure amplitude of one-third the mean chamber pressure. Again, it is shown that viscous effects favour the development of the transverse waves rather than longitudinal components. In the present experiments no evidence of high amplitude longitudinal waves was observed.

The mode identification just discussed depends in part on a knowledge of instantaneous perforation diameter. This parameter was obtained in the usual manner by assuming that the propellant mass consumed to time t was proportional to the pressure integral to the same time. The further assumption was made that the perforation remained cylindrical throughout the firing. Interrupted firings were made to check this procedure. The results of one such firing are shown in Figure 5. The motor was interrupted by nozzle blow-off alone. For this severely unstable motor the measured and computed values of the change in mean perforation diameter differ by less than two per cent. Further, the change in perforation diameter is relatively insensitive to axial and circumferential station.

Finally, visual inspection of the propellant surface after interruption revealed no gross irregularities. While the surface exhibited a fine scale roughness, no organized system of grooves or ridges was evident. On the basis of this fact and the lack of circumferential asymmetry it might be inferred that the local fluctuations of pressure and velocity should also be symmetric about the motor axis in which case the finite tangential travelling (so-called spinning) mode is indicated. The high frequency instrumentation suggests, however, that the active mode is a pseudo-standing wave-form wherein the orientation of the pressure nodal line fluctuates rapidly and somewhat randomly with time. It is clear that this latter mode form can produce uniform changes in mean burning rate. The tests conducted so far do not differentiate conclusively between the spinning mode and the statistically fluctuating standing mode, but favor the latter.

REPRODUCIBILITY OF THE EXPERIMENTS

We have so far discussed the detailed operation of a few unstable motors. These general features of operation will be taken for granted when we proceed to the results obtained from a large number of firings made over broad ranges of certain operating parameters. These latter results are significant only insofar as they could be repeatedly obtained in a reproducible manner. By reproducible is meant the repeatability of the P_c vs t curves for firings under identical conditions and the repeatability of the onset of instability. In the illustrative firing of Figure 2 the unstable increase in mean chamber pressure (P_c) corresponds to an increasing level of gaseous oscillations. It was characteristic of the firings that at some increased P_c the smooth unstable rise ceased. (See "break" point in Figure 2). After

these large deviations have occurred it should not be surprising should the character of the P_c vs t curves deviate widely from firing to firing. Actually there was a remarkable correspondence in the overall pressure-time behaviour of most firings made under identical conditions. Nevertheless there were many exceptional cases. Some of these deviations can be attributed to mechanical failure of the propellant grain structure. In others, the instability persisted at high levels for unusual periods of time.

On the other hand, the initial phase of the instability process (up to the break in the chamber pressure versus time curve) was in general remarkably reproducible. That is, the overall delay time from ignition to the break in the P_c vs t curves did not vary greatly for similar motors and the P_c values at the break, while somewhat scattered were on the whole quite consistent.

The reproducibility of unstable firings in this work is in contrast to most of the experience in this field. At the outset of the program it was not obtained despite the fact that the manufacturing controls exerted were those in standard usage and certainly adequate to obtain reproducible results in stable designs. The data obtained from early firings showed that reproducibility could be improved by extending the length of time allowed for the curing process. This effect is illustrated in Figure 6 where the P_c vs t curves for ten firings are shown, grouped in pairs. All motors were made using the same manufacturer's lots of raw materials. The paired motors were made from particular batches of propellant, were identical in geometry and were processed and fired under identical conditions. Batches R25, R28, and R26 were cured 72 hours at 160°F with the casting mandrel in place; received 32 hours at 160°F with the casting mandrel removed during the application of the end restrictor plugs; and received 24 hours at 160°F while completely assembled for firing, during a prefiring, temperature-conditioning period. It is clear that satisfactory in-batch reproducibility was not achieved.

However, an 89 hour cure, followed by the additional processing just described, produced the results shown for R27. In this case the firings are almost identical up to the break in the unstable rise in P_c . A further increase of cure time to 116 hours led to the firings of batch R24 which leave nothing to be desired insofar as in-batch reproducibility is concerned. Hence, it appears that the cure time must exceed some minimum value if in-batch reproducibility of unstable effects is to be attained. Furthermore, this time exceeds that necessary to obtain reproducible stable ballistics.

The time required to reach a particular state of overall cure should be more uniform for motors made from the same batch of propellant than for those made from different batches since manufacturing variations can enter more easily in the latter case. Furthermore, changes in manufacturer's lots of raw ingredients with attendant variation in their chemical nature could be expected to produce further changes in the necessary overall cure time. However, it was subsequently found that a cure of 120 hours with the casting mandrel in place plus 32 hours for restricting plus 48 hours additional was sufficient to produce reasonable uniformity of results in the remainder of the experimental program. To ensure that this was so, repetitions of earlier firings were made at intervals and the results compared. Finally, the very definite trends obtained when gross changes were made in many of the motor operating parameters are themselves a strong argument for the existence of controlled conditions.

EFFECT OF CHANGING THE PORT TO THROAT DISTANCE

Certain features of motor construction remained fixed in the exploratory firings. In particular the linear distance between the nozzle end of the grain (port) and the nozzle throat was essentially constant with only small variations due to the dependence of nozzle contour on throat diameter. In order to determine the effect of changing this dimension while keeping the remainder of the motor geometry fixed, three motors were made from the same batch of propellant using the designs shown in the left column of Figure 7. The grain length was fixed at 30.5 in. and throat diameter at 1.70 in. while the port to throat distances were approximately zero, 3.5 in. and 7.5 in. The P_c vs t curves shown in the figure are essentially the same in the three cases. Hence the instability process does not depend strongly on port to throat distance, at least at the particular operating conditions of these tests.

EFFECT OF RESTRICTOR PLUGS

A second feature of motor construction which remained unchanged in all firings was the use of restrictor plugs, one on each end of the grain. The plugs were made from a polysulfide base with curing additives but no oxidizer, and were cast and cured in position. During the firings, the head-end plugs remained essentially intact while the nozzle end plugs were for the most part badly eroded by the hot gas flow. To make certain that the plugs did not influence the instability process in some unknown manner, the three motors shown in the right column of Figure 7 were constructed and fired. One motor was constructed in the standard manner, the second with no nozzle end plug, and the third with no head-end plug. The absence of the plugs increased the ratio of burning surface area to throat area, K_n , by approximately 3.5 per cent at ignition and the pressure by a corresponding small amount. It is clear from the pressure-time curves that the plugs exerted little if any influence, at least at this operating point.

EFFECT OF CHANGING THE INITIAL GRAIN PERFORATION DIAMETER

As a result of the foregoing observations and rather extreme precautions taken in manufacture, assembly and firing, it is believed that the experimental trends that follow are indicative of the gross features of the instability mechanism and not of random influences in manufacture. The experiments reported here were conducted solely for the purpose of elucidating the instability mechanism, in the sense that the results give trends that any adequate theory must reproduce.

In order to quickly become familiar with the type of results obtained, consider the effect of firing a series of stable motors, identical in every respect except that the initial perforation diameter, D_{p1} , is increased for successive firings. Ideally, this is equivalent to repetitive interruption and restarting of the motor with smallest D_{p1} . Hence the stable pressure time curves could be superimposed and the time axis converted to equivalent D_p . When this was done with unstable motors the results shown in

Figure 8 were obtained. Here we should confine our attention to the parts of the firings up to the "break" point since after this point the P_c vs t curves were frequently distorted due to severe grain damage. We may consider jointly the two series shown, since they differ only in the nozzle size used and the trends are identical. In every firing an overall delay occurs between ignition and maximum instability. Maximum instability does not occur at the same D_p and therefore not at the same frequency. Furthermore, maximum instability for a particular firing can occur at a diameter corresponding to the initial stages of instability in a motor with somewhat larger D_{p_i} . Also, as was indicated earlier, the motors appear to be stable for a few tenths of a second after ignition. This does not preclude a motor of smaller D_{p_i} from being severely unstable at equivalent diameter. Thus it may be concluded that the stable delay period does not represent a situation in which instability is prohibited by improper relationship between frequency and any conceivable time lag associated with quasi-steady combustion. Alternatively, it is not entirely clear that unsteady conditions associated with ignition should persist for times on the order of tenths of seconds. Finally, in these and other firings instability has been observed over the frequency range corresponding to roughly $D_p = 1.5$ to 6.0 in. These diameters correspond to frequencies in the fundamental tangential mode ranging from approximately 14.5 kc to 3.6 kc. The range was limited only by the size of the motors fired and it is probable that excitation can occur over a broader band of frequencies than was verified experimentally. Within this band no evidence of frequency-selective excitation was observed.

The situation is further complicated by an effect illustrated in a third series of firings shown in Figure 9. The firing with $D_{p_i} = 1.90$ in. became weakly unstable after a short stable delay period and remained weakly unstable until approximately $t = 2.5$ sec. The firing with $D_{p_i} = 2.08$ in. shows the beginning of a rapid unstable rise which however was limited. The magnitude of the instability at the break was somewhat greater than at the corresponding point of operation of the $D_{p_i} = 1.90$ in. motor. The 2.28 in. motor was several times as unstable at the break as the 2.08 in. motor at the same diameter.* It thus appears that the degree of instability at a particular geometrical configuration depends on the preceding pressure-time history of the firing. In particular, the results indicate that the tendency towards high amplitude instability at given operating point is inhibited by a preceding period of combustion and/or low level oscillation.

The remainder of the experiments to be discussed involved many motors placed in operation from a variety of initial conditions. The experiments just described emphasize the importance of keeping in mind the fact that the behaviour of a motor at given instantaneous geometry is not the same as that of another motor which reaches the same geometrical configuration at some time in its firing but which started from different initial conditions. For this reason the firings to be discussed will be referred to in terms of their initial conditions. That is, a complete initial geometrical specification of each motor, as well as the initial grain temperature will be given for each firing.

* Partial grain break-up occurred in the 2.28 in. motor and produced the severe pressure peak just after the break.

EFFECT OF CHANGING THE PRESSURE OPERATING LEVEL

Several series of motors were fired in which the initial value of Dp , Dp_i was fixed as were the grain length Lp and the grain temperature Tp . Two series are shown in Figure 10. Five firings are shown for which $Dp_i = 2.45$ in., $Lp = 31$ in., and $Tp = 160^\circ F$. These motors were fired with nozzle sizes ranging from 1.70 in. to 1.35 in. As a result the initial value of the ratio of burning surface to nozzle throat area, Kn , ranged from 109 to 174 and the initial operating pressure from approximately 180 psia to 325 psia.* Several features of the firings are immediately apparent. The most striking perhaps, is the degree of instability exhibited. As the initial value of Kn (pressure) was increased by reduction of nozzle throat size in successive firings of otherwise similar motors, the degree of instability increased. However, this trend did not continue indefinitely. An increase of Kn_i from 140 to 156 resulted in a sharp transition from a strongly unstable motor to a weakly unstable motor. A further increase of Kn_i to 174 led to a completely stable firing. This same trend has been confirmed for motors of several different initial values of Dp . The results obtained for $Dp_i = 2.8$ in. are also shown in Figure 10. If we call the mean pressure at the break \bar{P}_B and the pressure which should have existed at this value of Dp had the firing been stable P_{c_s} , then the ratio $(\bar{P}_B - P_{c_s})/P_{c_s} \equiv \Delta \bar{P}_c/P_{c_s}$ is a measure of the degree of instability of a particular firing. In general P_c and the oscillation amplitude showed the same close correlation exhibited in Figure 3, hence ΔP_c is also a measure of oscillation amplitude. A plot of $\Delta P_c/P_{c_s}$ vs Kn_i is given in Figure 11 for firings made with values of Dp_i ranging from 2.2 in. to 3.0 in., all with $Lp = 31.0$ in. and $Tp = 160^\circ F$. The firings shown in Figure 10 are included among these. It is clear that near $Kn_i = 150$ the behaviour of the motors depended critically on chamber pressure level. That is, for given Dp_i a change in nozzle size of only a few per cent was sufficient to produce a remarkable transition from maximum instability to very weak

* During stable combustion the propellant burned according to the empirical non-erosive law

$$r_s = a P_{c_s}^n$$

where r_s is the stable linear burning rate, a and n are constants at given grain temperature and P_{c_s} is the stable chamber pressure. The stable chamber pressure is related to motor geometry by

$$P_{c_s} = (a \rho_p c^* Kn)^{\frac{1}{1-n}}$$

if length and dissipative effects are neglected. Here ρ_p is the propellant density and c^* the propellant characteristic exhaust velocity.

For the cylindrical motors Kn is given by

$$Kn = \frac{4DpLp}{d_t^2}$$

instability. On the other hand the operating pressure level had to be increased considerably further in order to entirely suppress the unstable tendency.

FURTHER EXPERIMENTS VARYING INITIAL PERFORATION AND NOZZLE DIAMETERS

In view of the dependence of the instability on pressure-time history, it was necessary to fire a large number of motors covering various initial values of D_p and Kn . The results of these firings for $L_p = 31.0$ in. and $T_p = 160^\circ\text{F}$ are shown in Figure 12. The points plotted represent initial conditions of Kn vs D_p for the firings. Lines of constant throat diameter, d_t , are indicated for $L_p = 31.0$ in. The change in Kn and D_p during a particular firing is obtained by following the appropriate d_t line. For example, the firing with initial condition $D_p = 3.05$, $Kn = 105$ proceeded along the d_t line, $d_t = 1.895$ in. out to $D_p = 5.0$ in. which was the ID of the motor case.

Several features of the plot are immediately apparent. The Kn - D_p plane may be divided into two major regions; a stable region and an unstable region. Motors with initial conditions which lie in the stable region operated stably throughout their firings. The unstable region refers to motors which were unstable during at least a portion of their pressure-time histories.

The stable region is separated from the unstable region by a line which we will call the stability limit. For values of D_p greater than 2.3 in., the stability limit is a line of constant d_t . It will be shown that it is in general a line of constant L_p/d_t^2 with the value in this case corresponding to $L_p = 31$ in. and $d_t \approx 1.37$ in. For D_p less than 2.3 in. the stability limit curves upward to some extent. In this region the firings were increasingly erosive but it is not known whether this accounts for the deviation. The significance of the stability limit is emphasized by the fact that the unstable firings on the $d_t = 1.30$ and 1.35 in. lines were unstable only in the very early part of the runs and quickly became stable after entering the stable Kn - D_p region.

The character of the unstable region in Figure 12 may be made clear by reference to the firings of Figure 10. These firings lie on the ordinates $D_{p_i} = 2.45$ and 2.80 in. It is seen that the unshaded region labelled weak region corresponds to firings at pressure levels greater than the critical level at which maximum instability occurs. The initial conditions for firings of maximum instability lie on the line labelled $\text{Max } \Delta P_c/P_{c_s}$. For brevity this line will be called the transition line. The nature of the trend shown in Figures 10 and 11 indicates that motors operating below the transition line and at sufficiently low pressure (i.e. small enough Kn_i or large enough d_t) should perhaps be stable. However, the low pressure limit of the propellant prevented experimental verification of this. Attempts to fire at extremely low pressures led to chuffing.

It is interesting to note that the transition line converges on the stability limit line near $D_p = 2.3$ in. In this region a very small increase in throat diameter is sufficient to transform a stable design to

one that is severely unstable. The abrupt nature of this change and of that occurring all along the transition line perhaps accounts for the apparently random occurrence of instability during some development programs. Presumably a marginally stable design could become strongly unstable due to the effect of manufacturing variations on the location of these lines. Here it is of course assumed that a similar system of stable, unstable regions exists for motors of differing grain cross-section. This has not yet been conclusively demonstrated experimentally although available data indicates that it is very likely.

In addition to the 5 x 31.5 in. motors, several others with a variety of case inside diameters and lengths were fired at 160°F. These motors were intended to check the instability trends already established with the 5 x 31.5 in. motors. The Kn_i vs Dp_i plots are given in Figure 13. The stability limit and transition lines for the 5 x 31.5 in. motors are shown in the same figure. The motors with nominal $Dp_i = 0.5, 1.0, \text{ and } 1.2$ in. were stable. Reference to Figure 13 shows that they probably lie above the stability limit for the 31 in. motors. Two firings were made with $Dp_i = 1.5$ in. One was stable and one unstable. In Figure 13 it may be seen that the initial conditions were in good agreement with the stability limit for the 31 in. motors. This agreement was obtained in spite of the fact that the two sizes of motors differ greatly in grain length, case inside diameter and web thickness. Several firings were made with 3 x 5 x 38/38.5 in. and 3 x 5 x 44.5/45 in. motors. The same trends were observed as for the 31 in. motors and the stability limit is in good agreement. Finally, several motors were fired with 6 in. inside diameter cases. Once again agreement was obtained. Hence the experimental results strongly indicate that the stability limit depends only on the perforation diameter and the Kn ratio at the operating point. This may be restated as follows: The acoustic frequencies characteristic of the perforation cavity depend primarily on the cavity diameter. The quasi-steady chamber pressure and burning rate depend primarily on Kn . Hence, the stability limit is believed to be determined by the interrelation between the active acoustic mode and the combustion mechanism, without regard to such factors as web thickness, case diameter, and grain length.

It is also informative to examine Figure 13 to determine the effect of linear scale-up. Since Kn is non-dimensional it remains constant during linear scale-up. Hence the initial operating point moves to the right along a line of constant Kn . It is clear that a stable design is very likely to scale into the unstable region if the scale factor is great enough. However, since motors of very large cross-section were not tested, it is uncertain whether further stable regions exist at large values of perforation diameter. Hence it may be possible to by-pass the unstable region by scaling sufficiently.

EFFECT OF GRAIN TEMPERATURE

A fixed initial grain temperature of 160°F was used for all the firings of Figures 12 and 13. The number of motors required to repeat the complete set of firings over a range of grain temperatures was prohibitive. In order to obtain some idea of how the stability limit and transition lines change location as a function of grain temperature, a series of 42 cylindrical motors with $Dp_i = 3.0$ in. and $L_p = 31$ in. was fired over the grain temperature range -80°F to 180°F. The initial pressure level was determined for stable

operation and transition operation at nine different grain temperatures. Hence the intersection points of the $D_p = 3.0$ in. ordinate with the stability limit and transition lines in the Kn - D_p or equivalent Pc_s - D_p plane (see Figure 14) were determined as functions of grain temperature. The results may be visualized as a cross-section of the stability limit and transition surfaces in the Pc_s - D_p - T_p coordinate system. This cross-section is shown in Figure 15 where the initial conditions of the firings are plotted in the initial chamber pressure versus grain temperature plane. During and immediately after ignition, the motors were not in quasi-steady operation, hence the pressure during this interval was subject to large deviations from normal. Inspection of reduced data led to the conclusion that by the time $D_p = 3.15$ in., the motors were in quasi-steady operation and at the same time had not entered instability. Since it was desirable to compare the operation at a condition of fixed geometry, the operating pressure at $D_p = 3.15$ in. was chosen for the initial pressure reference condition.

It is clear from Figure 15 that both the stability limit and transition surfaces shift to lower pressure levels as the grain temperature is decreased from 160°F . The profiles of these surfaces cross over those of constant nozzle size as shown, therefore, a motor of entirely fixed geometry fired over a range of grain temperatures can behave in a variety of ways depending on throat size. As an example consider the two series of firings shown in Figure 16. The left hand series of $d_t = 1.60$ in. and $Kn_i = 149$ was fired over the range of temperature -80°F to 180°F . The firings at 180°F and 160°F were strongly unstable, those from 140°F to 80°F mildly unstable, from 20°F to -40°F , stable, and unstable at -60°F and -80°F . Hence these motors follow the well known trend of being unstable at the temperature extremes. However, the right hand series shows that if the throat size is increased to 1.80 in. all firings lie below the stability limit surface and are unstable.

At each grain temperature the instability showed similar dependence on operating pressure level in that stable, weakly unstable and strongly unstable regions of operation existed. The critical levels for stability and maximum instability decreased with temperature down to approximately -20°F . Below -20°F there is some indication that they may rise to higher levels. As noted earlier these profiles cross over those of constant nozzle size. The latter are determined by the dependence of the stable burning rate on grain temperature. Thus the dependence of the limiting surfaces on grain temperature is different from that of the stable burning rate. Finally, it should be noted that the maximum degree of instability attainable at given grain temperature also decreased with temperature at least to approximately 0°F .

EFFECT OF GRAIN LENGTH

A number of experiments were performed to investigate the effect of grain length on the instability process. The motors used had 3.0 in. initial port diameters. A series of firings was made at $T_p = 160^\circ\text{F}$ with grain lengths of 17, 31, 38 and 44.5 in. and with $Kn_i = 130$. Representative pressure-time curves are shown in Figure 17. A plot of $\Delta Pc/Pc_s$ vs L_p for these firings is shown in Figure 18. It is clear that the degree of instability at fixed Kn_i was independent of grain length for grain lengths greater than 31 in. On the other hand, the instability became markedly weaker

when the grain length was reduced from 31 in. to 24 in. while 17 in. motors were only weakly unstable. Hence a critical grain length lying between 24 and 31 in. existed for the 3.0 in. motors, below which the instability decreased rapidly with decreasing grain length. Further experiments were performed with the 17 and 24 in. motors in which the operating pressure level was decreased (i.e. $Kn_i < 130$) in successive firings. For both lengths the motors became less unstable indicating that the firings at $Kn_i = 130$ were below the transition level. However, a firing at $Kn_i = 147$ with the 24 in. motor was stable indicating that the stability limit was exceeded in this case. Since the stability limit is at approximately $Kn_i = 200$ for the 3 x 5 x 31/31.5 motor (see Figure 12) it would appear that the stability limit has changed as a function of grain length. However, it has been shown earlier in connection with Figure 13 that this is in general, not the case and that it is probably true that the stability limit depends only on the interaction between the oscillation frequency and the burning mechanism of the propellant. A more likely explanation for the behaviour of the 17 and 24 in. motors appears to be in an unfavorable increase in the losses of the system, as compared to the driving energy input. That is, it is assumed that the losses were so great as to reduce the instability below detection level at values of Kn_i less than those corresponding to the true stability limit.

Alternatively, it may be postulated that a certain coupling must exist between the tangential mode and the longitudinal mode associated with the axial dimension of the motor. The available evidence argues against this. The experiments discussed in connection with Figure 7 may be cited. There the motor length was changed while the grain length was maintained constant. Thus if an axial dimension is important frequency-wise it is probably the grain length. But in fact, no high amplitude driving in axial modes was ever noted. As was discussed earlier, only the high frequency transverse oscillations were driven to large amplitude. Thus it is assumed that increased damping is the more likely explanation of the two.

MOTORS WITH OPPOSED-PLANE GRAIN DESIGNS (Slab Type Motors)

In addition to the cylindrical motors, two designs of slab-type motors were fabricated and fired. These designs are shown in Figures 19 and 20 and will be designated Type 1 and Type 2, respectively.

Two firings were made with the Type 1 motor. The pressure-time curves are shown in Figure 21. Due to the grain configuration, the operating pressure remained essentially constant for a period of time and then began a slow tail-off. The firing at the higher initial pressure was stable. The firing at the lower operating pressure was unstable in the sense that gaseous oscillations occurred. However, no deviations in the mean operating pressure were noted as would have been the case had the motor been of the cylindrical type. The frequency of oscillation decreased with time and agreed with the acoustic value for the transverse fundamental sloshing mode. In this mode the gas moves only in a direction perpendicular to the burning surface; no motion of the gas tangential to the burning surfaces takes place.

The Type 2 slab motors were based on trends observed in concurrent

firings with the cylindrical motors. The grain length was increased from the Type 1 length of 23.5 in. to approximately 38.5 in. in the Type 2 motors. The steel inserts used in the Type 1 motor were omitted, hence the Type 2 motors burned with a regressive pressure-time curve from ignition onward. This, together with an increase in spacing between the grain surfaces to 1.8 in. permitted the longer motors to be fired at lower pressures without choking of the flow in the grain port. A series of six firings with the Type 2 slab motor is shown in Figure 21.

The firings using Type 2 slab motors covered a range of Kn_i from 84 to 219 by choice of a suitable range of nozzle throat diameters. Only the firing with the highest value of Kn_i was stable. The remaining firings at lower Kn_i all exhibited gaseous oscillations in the fundamental transverse mode similar to those found in the Type 1 slab motor. The peak-to-peak magnitude of these oscillations was as large as 20 per cent of the average chamber pressure. No changes of mean pressure were observed. It is quite certain on the other hand that tangential pressure oscillations of these magnitudes would have produced easily detectable changes in the average burning rate of the propellant.

In this connection it is interesting to note that in a resonating cavity, a solid boundary is subjected to pressure oscillation whether the gas motion be normal or tangential to the surface. In a local region of grain surface the two modes of oscillation should be indistinguishable insofar as pressure effects are concerned. On the other hand, at the solid surface the gas velocity is zero for the normal oscillations but definitely non-zero for the tangential mode. These tangential velocity components may become of considerable magnitude and it appears that they may be a significant influence in affecting the propellant burning rate. The conclusion may possibly be made that while the pressure fluctuations themselves are responsible for their own excitation, it is the corresponding tangential velocities induced by them that augment the propellant burning rate. The contrast between results obtained in cylindrical motors and slab motors certainly supports such a conjecture.

CONCLUSIONS AND CONCLUDING REMARKS

By extremely careful control of the propellant manufacturing procedure and by extending the cure time to nearly twice its normal length, it has been possible to secure results of rocket firings that are almost completely reproducible with regard to the occurrence of unstable burning and early phases of variation of mean chamber pressure with oscillation amplitude. A total of over 250 research firings using case-bonded cylindrically perforated motors were made under these conditions along with about 150 additional ballistic firings. The results summarized below are based upon these firings. All firings were made with a given ammonium perchlorate-polysulfide propellant the composition of which was carefully controlled during the research period.

Detailed measurement of oscillatory frequencies confirmed the fact that the first tangential mode was providing the excitation and was associated with the instability. The variation of frequency with grain perforation diameter was that to be expected from acoustic theory

in spite of the fact that at times the peak oscillating pressure reached half of the mean chamber pressure. Axial oscillations were present but were weak and obviously not contributing to the excitation even though the motor length was varied by a factor of more than two and one-half.

At given grain temperature, stable firings with the cylindrical motors exhibit a progressive pressure-time curve. The chamber pressure increases with Kn , the ratio of burning surface area to nozzle throat area, as the perforation diameter D_p becomes greater due to burning. In the Kn - D_p plane there existed regions of stable, mildly unstable and severely unstable combustion as defined by firings of motors with 31 in. grain length. For sufficiently high values of Kn , the combustion was stable regardless of D_p . At lower values of Kn the motors were weakly unstable. The dividing line between these regions in the Kn - D_p plane increased essentially linearly with D_p and was very nearly a line of constant nozzle size. As Kn was reduced further the instability became very gradually stronger until at a critical value of Kn the motors suddenly became severely unstable. The line of maximum instability intersected the upper stability line at a low value of D_p and gradually increased in Kn level as D_p increased from this point. The region below the line of maximum instability was characterized by a gradual decrease in the severity of the instability as Kn was reduced from the critical value.

A reduction of grain length below 31 in. to 17 in. successively reduced the severity of the instability at a given operating pressure level. An increase of grain length from 31 in. to 44.5 in. did not affect the degree of instability at a given operating level; nor did the upper stability line change.

The effect on the upper stability line and the lines of maximum instability of changing the initial grain temperature was determined for motors of 3 in. initial perforation diameter and 31 in. grain length, fired over the temperature range -80°F to 180°F . Both lines moved to lower pressure levels as the grain temperature was decreased but the reduction was not the same as that due to grain temperature effects on the burning rate. The results are in agreement with the observation that motors with fixed geometry fired over a range of grain temperatures can exhibit instability at the temperature extremes and yet operate stably at medium temperatures. Furthermore, the three instability regions described earlier existed at all grain temperatures.

Slab motors with opposed-plane grain surface exhibited oscillations in the fundamental transverse mode. The peak-to-peak magnitude of these oscillations were as large as 20 per cent of the chamber pressure, yet no effect on the mean burning rate was observed. In the cylindric motor, pressure oscillations of this magnitude showed a strong effect on the burning rate. Hence it is concluded that the tangential velocities associated with the tangential mode were largely responsible for modification of the burning rate.

Measurement of the fluctuating pressures in the cylindric motors and grain inspection after interrupted firings suggested that the mode of oscillation was the fundamental standing tangential mode. The orientation of the pressure node line appeared to change in a random manner and did not spin at the frequency of oscillation as in the travelling tangential mode.

While these results were obtained through the use of a particular propellant and grain design it seems reasonable to suppose that the trends noted are qualitatively applicable to other motors with similar acoustic properties, provided such motors operate in an instable manner.

NOMENCLATURE

a	Ballistic parameter in burning rate law $r_s = aP_c^n$
A_b	Area of the burning surface of propellant grain
a_c	Speed of sound inside rocket motor
A_t	Area of nozzle throat
c^*	Propellant characteristic exhaust velocity
D_p	Diameter of the motor port or perforation
d_t	Diameter of the nozzle throat
f	Frequency of gaseous oscillations
Kn	Ratio A_b/A_t
L_p	Length of the propellant grain
n	Ballistic parameter in burning rate law $r_s = aP_c^n$
P_{ac}	Peak-to-peak amplitude of gaseous oscillation
\bar{P}_c	Mean value of the unstable chamber pressure
\bar{P}_{c_B}	Value of \bar{P}_c at the "break" in the \bar{P}_c vs t curve (See Figure 2)
P_{c_s}	Stable value of the chamber pressure
r_s	Stable linear burning rate of propellant
R_p	Radius of the motor port or perforation
t	Time from ignition
T_p	Prefiring temperature of the propellant
$\bar{\gamma}$	Average value of ratio of specific heats
Γ'	Related to $\bar{\gamma}$ through $\Gamma' = \bar{\gamma} \left(\frac{2}{\bar{\gamma} + 1} \right)^{\frac{\bar{\gamma} + 1}{2(\bar{\gamma} - 1)}}$
$\Delta \bar{P}_c$	$\Delta \bar{P}_c \equiv \bar{P}_{c_B} - P_{c_s}$
ρ_p	Density of propellant

NOMENCLATURE - continued

Subscripts

h	Head end of motor
i	Value at ignition
n	Nozzle end of motor
s	Stable
t	Throat

REFERENCES

1. Boys, S.F., and Schofield, A.; "Studies Accessory to the Development of Classified Rockets", Woolwich Arsenal, England, (1942)
2. Wimpess, R.N., "Internal Ballistic of Solid-Fuel Rockets", McGraw-Hill, N.Y. (1950)
3. Smith, R.P. and Sprenger, D.F., "Combustion Instability in Solid Propellant Rockets", Proceedings of the Fourth Symposium (International) in Combustion. Williams and Wilkins, Baltimore, (1953) pp. 893-906
4. Grad, H., "Resonance Burning in Rocket Motors", Communications on Pure and Applied Mathematics, (1949), Vol. 2, No. 1
5. Cheng, S.I., "High Frequency Combustion Instability in Solid Propellant Rockets", Parts I and II, Jet Propulsion (1954), Vol. 24, pp. 27-32, pp. 102-109
6. Green, Leon Jr., "Some Properties of a Simplified Model of Solid-Propellant Burning", Jet Propulsion, (1958), Vol. 28, pp. 386-392
7. Nachbar, W., and Green, L. Jr., "Analysis of a Simplified Model of Solid Propellant Resonant Burning"., Lockheed Aircraft Corporation Report No. LMSD-5003 (1958)
8. Hart, R.W., and McClure, F.T., "Combustion Instability: Acoustic Interaction with a Burning Propellant Surface", The Johns Hopkins University, Applied Physics Laboratory Report TG-309, (October 1958)
9. Green, Leon Jr., "Observations on the Irregular Reaction of Solid Propellant Charges", Jet Propulsion, (1956), Vol. 26, pp. 655-659
10. Price, E.W., and Sofferis, J.W., "Combustion Instability in Solid Propellant Rocket Motors", Jet Propulsion, (1958), Vol. 28, pp. 190-192
11. Green, Leon Jr., "Some Effects of Oxidizer Concentration and Particle Size on Resonant Burning of Composite Solid Propellants", Jet Propulsion, (1958), Vol. 28, pp. 159-164
12. Green, Leon Jr., "Some Effects of Charge Configuration in Solid Propellant Combustion", Jet Propulsion, (1958) Vol. 28, pp. 482-485
13. Rogers, D.E. and Marble, F.E., "A Mechanism for High-Frequency Oscillation in Ramjet Combustors and Afterburners", Jet Propulsion, (1956), Vol. 26, pp. 456-462
14. Stott, Russel F., "A Ten-Band Spectrum Analyzer for Combustion-Stability Studies" presented at ARS Semi-Annual Meeting, Los Angeles, Calif. (1958)
15. Maslen, Stephen H. and Moore, Franklin K., "On Strong Transverse Waves Without Shocks in a Circular Cylinder", Journal of the Aeronautical Sciences, (1956) pp. 583-593

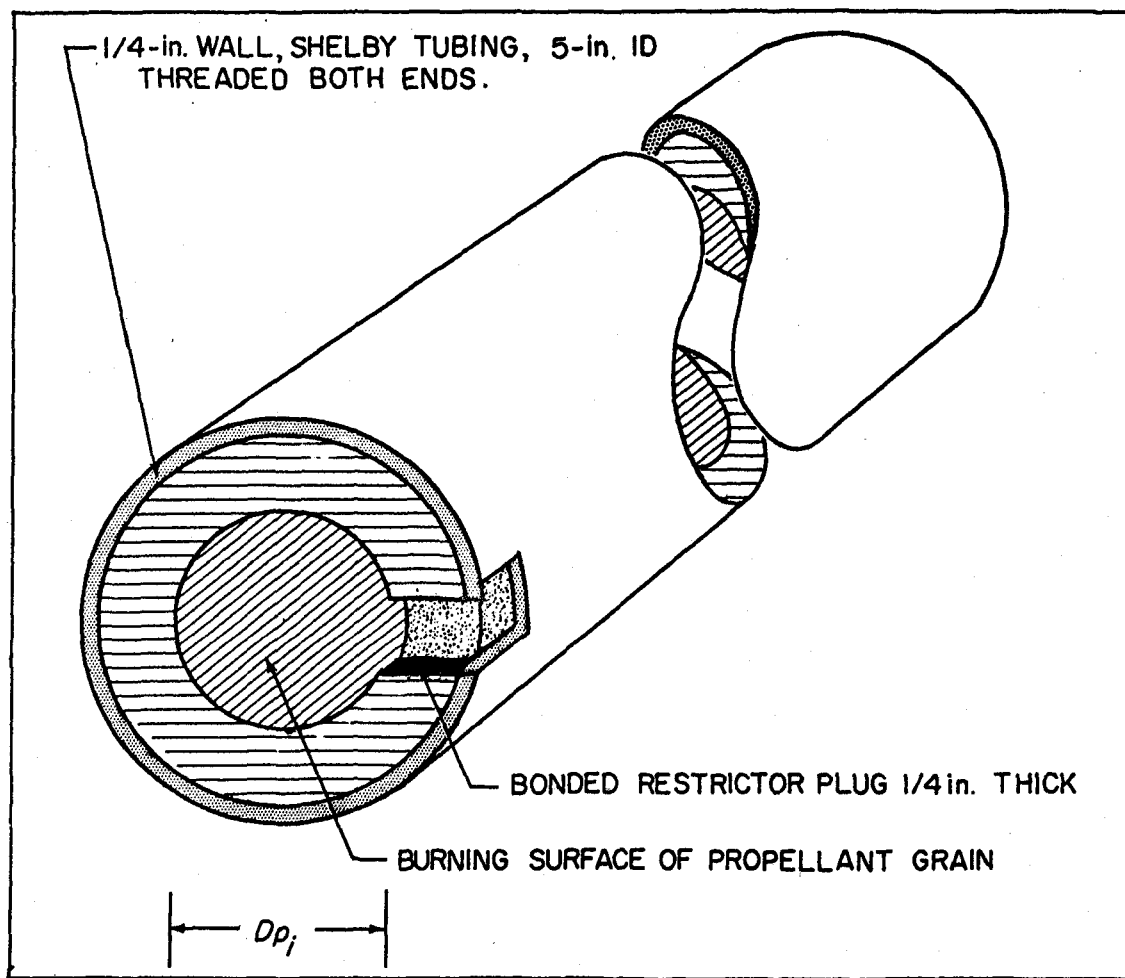


Figure 1. Cylindrical Motor Configuration.

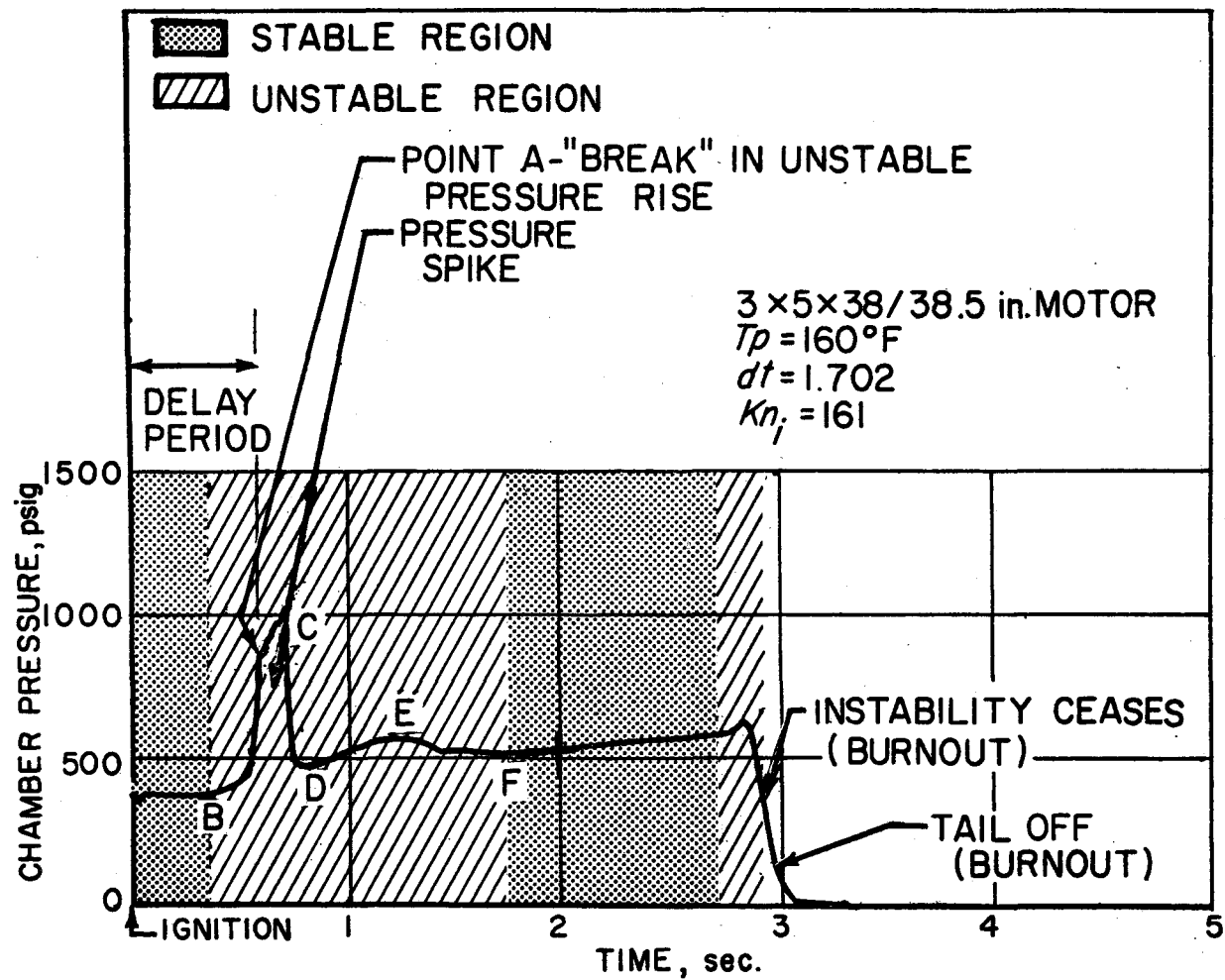


Figure 2. Mean Chamber Pressure, Time History of Typical Unstable Firing.

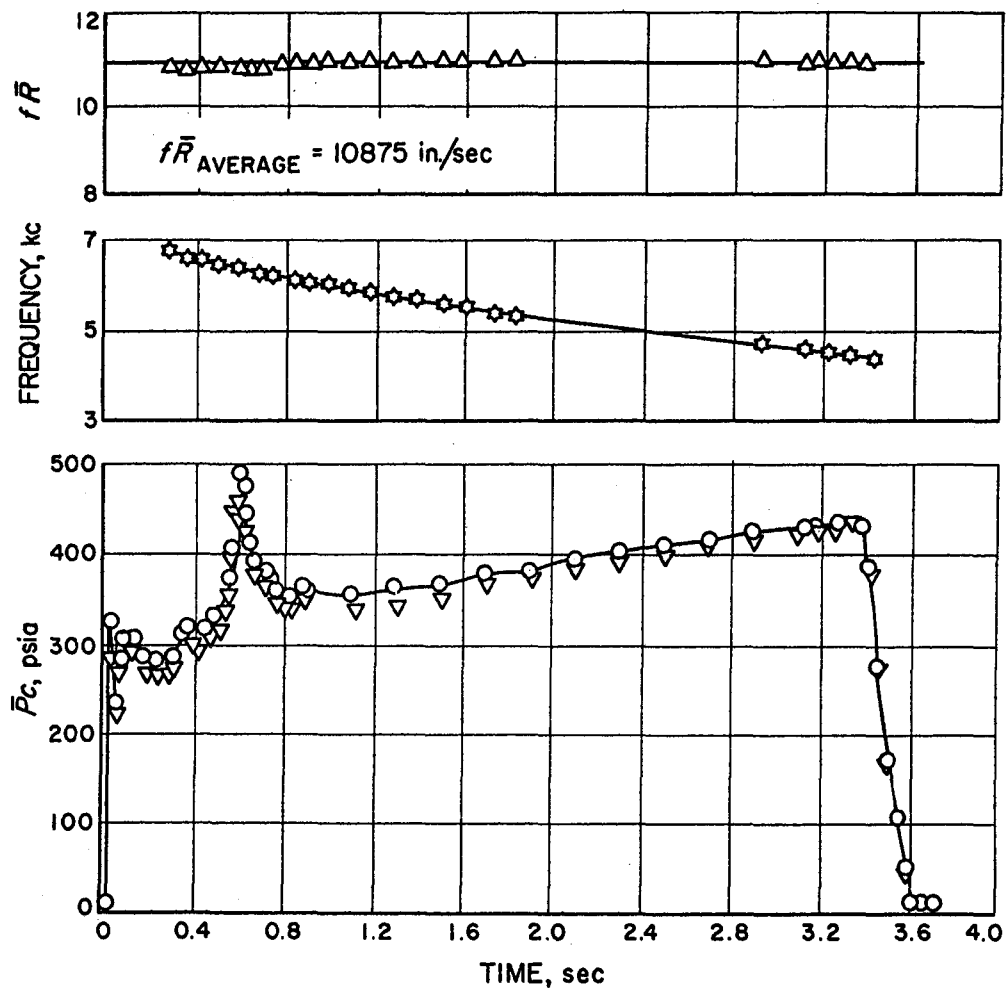


Figure 4. Typical Mean Chamber Pressure, Fundamental Frequency and Fundamental Frequency Times Instantaneous Radius, Versus Time History.

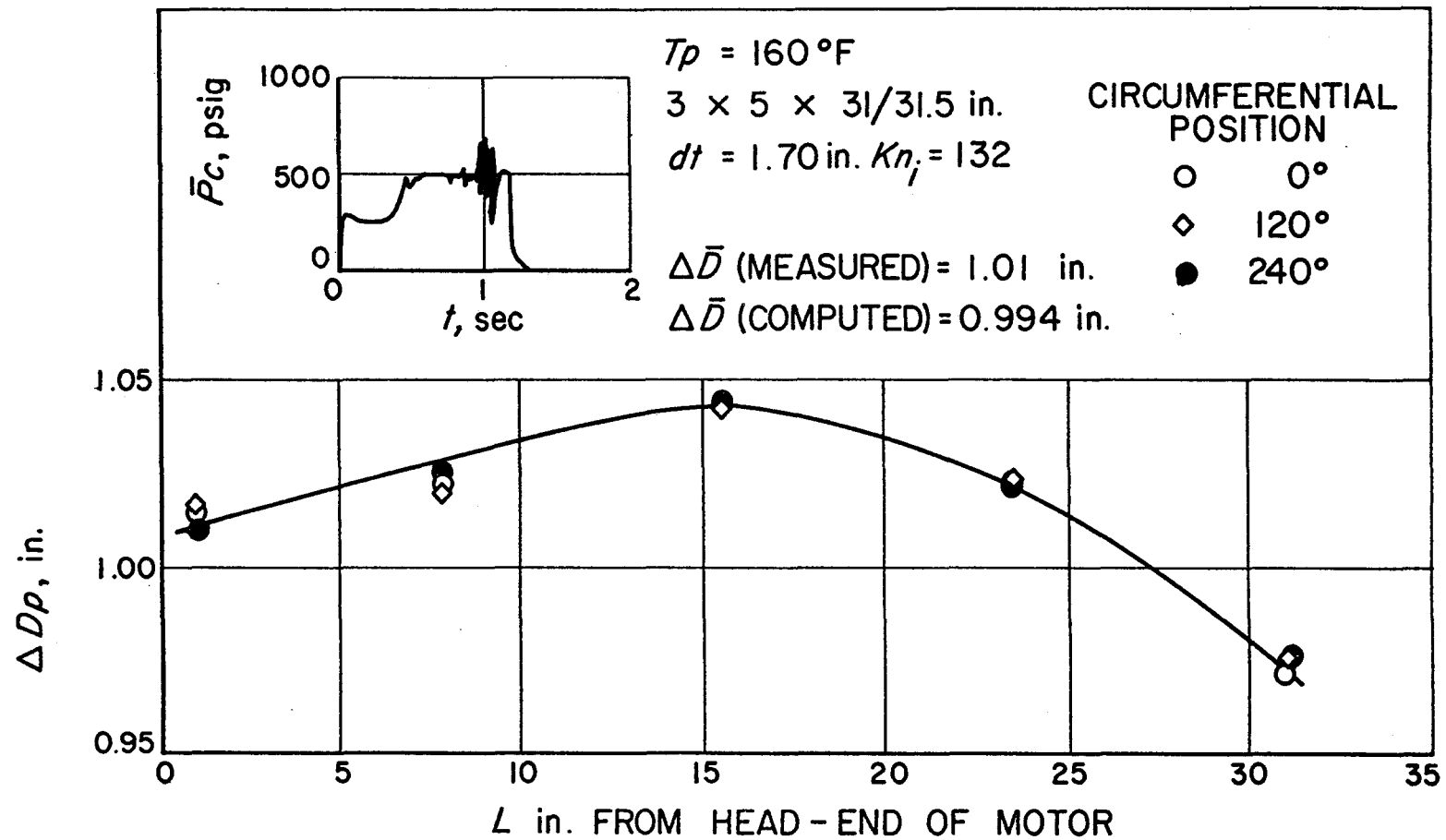


Figure 5. Change in Perforation Diameter Versus Length;
Self Interrupted Firing.

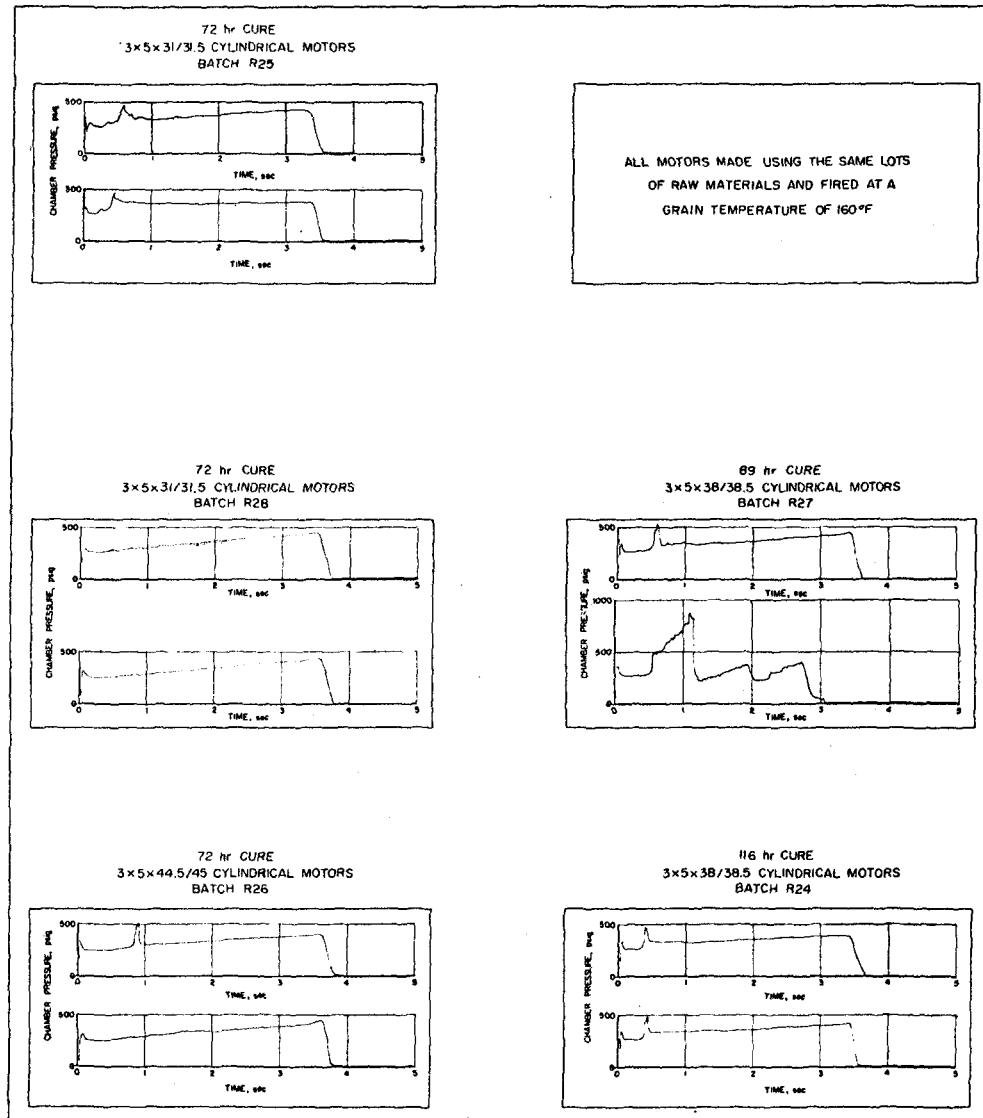


Figure 6. Effect of Cure Time on In-Batch Reproducibility.

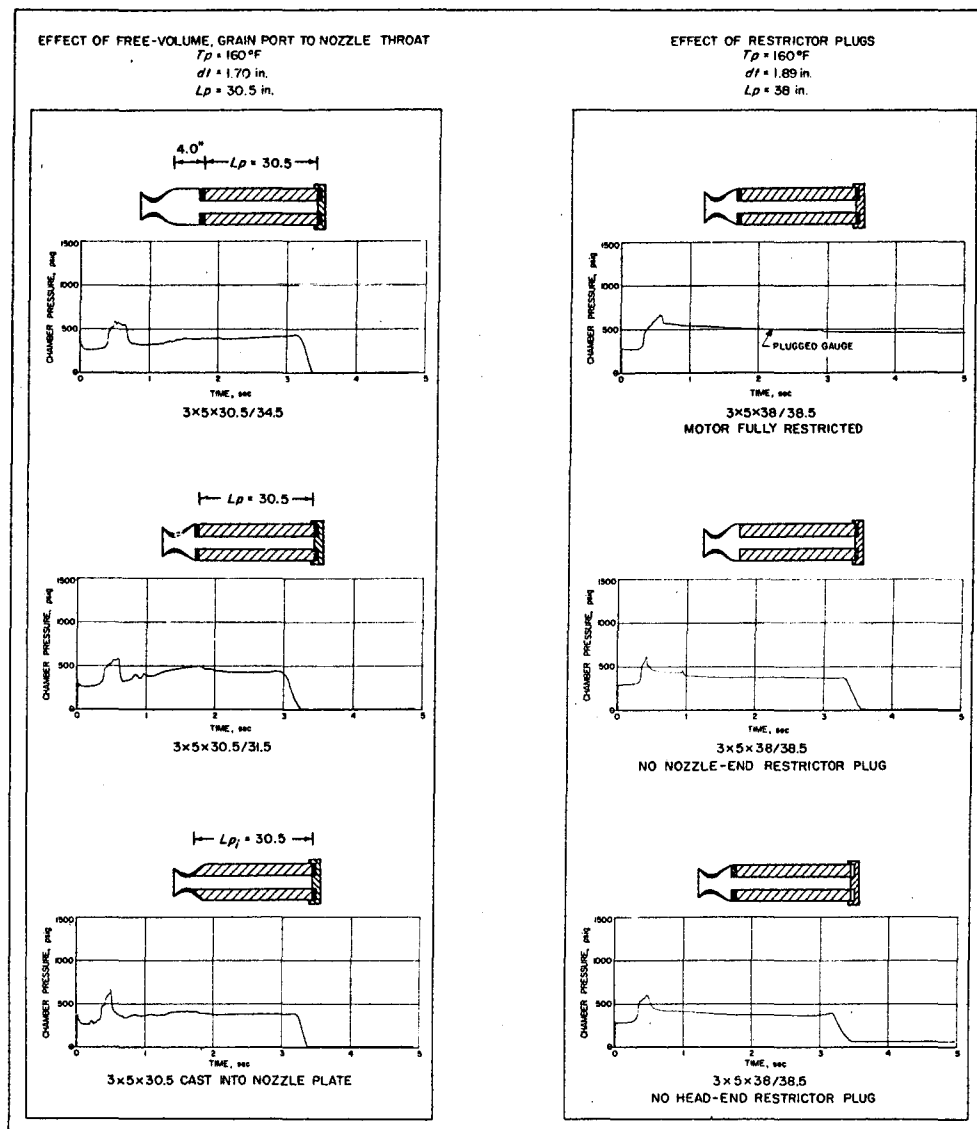


Figure 7. Effect of Varying Distance From Grain Port to Nozzle Throat; Effect of Removing Restrictor Plugs.

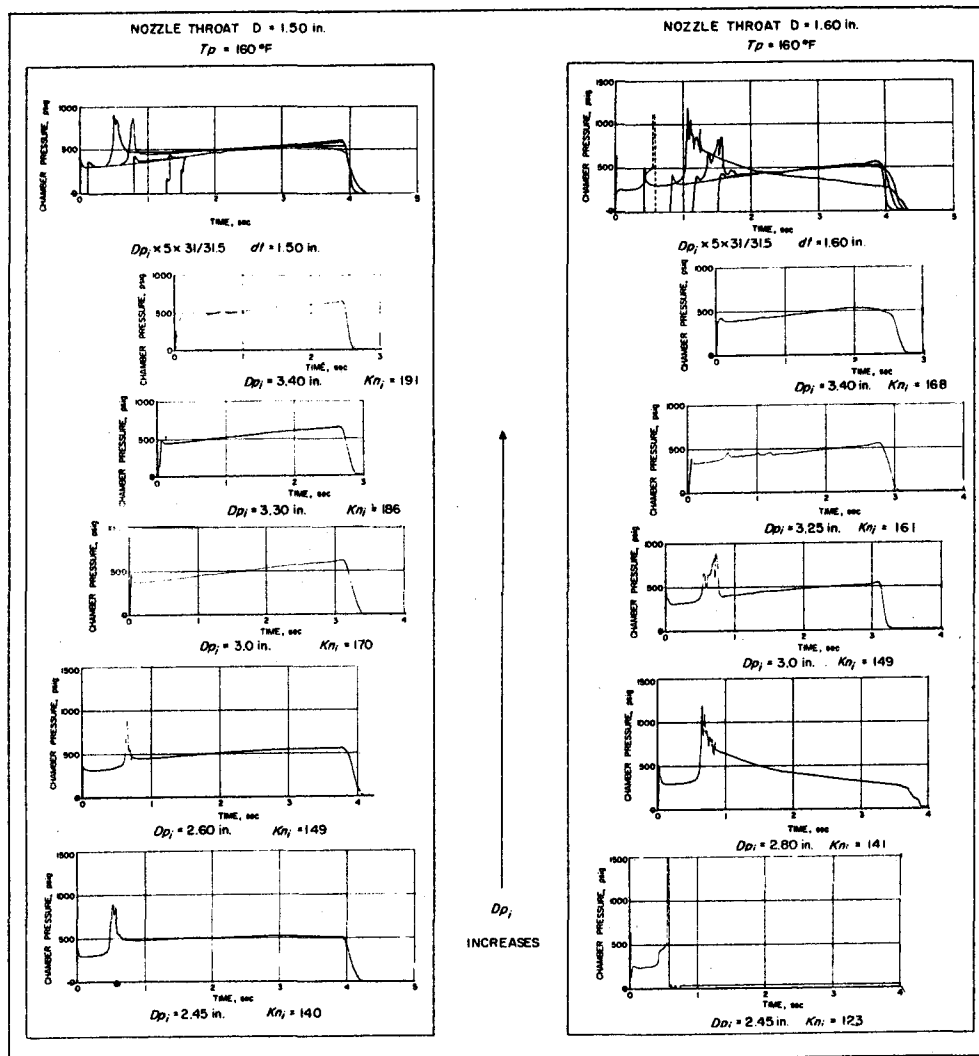


Figure 8. Effect of Varying Initial Port Diameter with Otherwise Fixed Geometry; Nozzle Throat Diameter = 1.50 and 1.60 in.

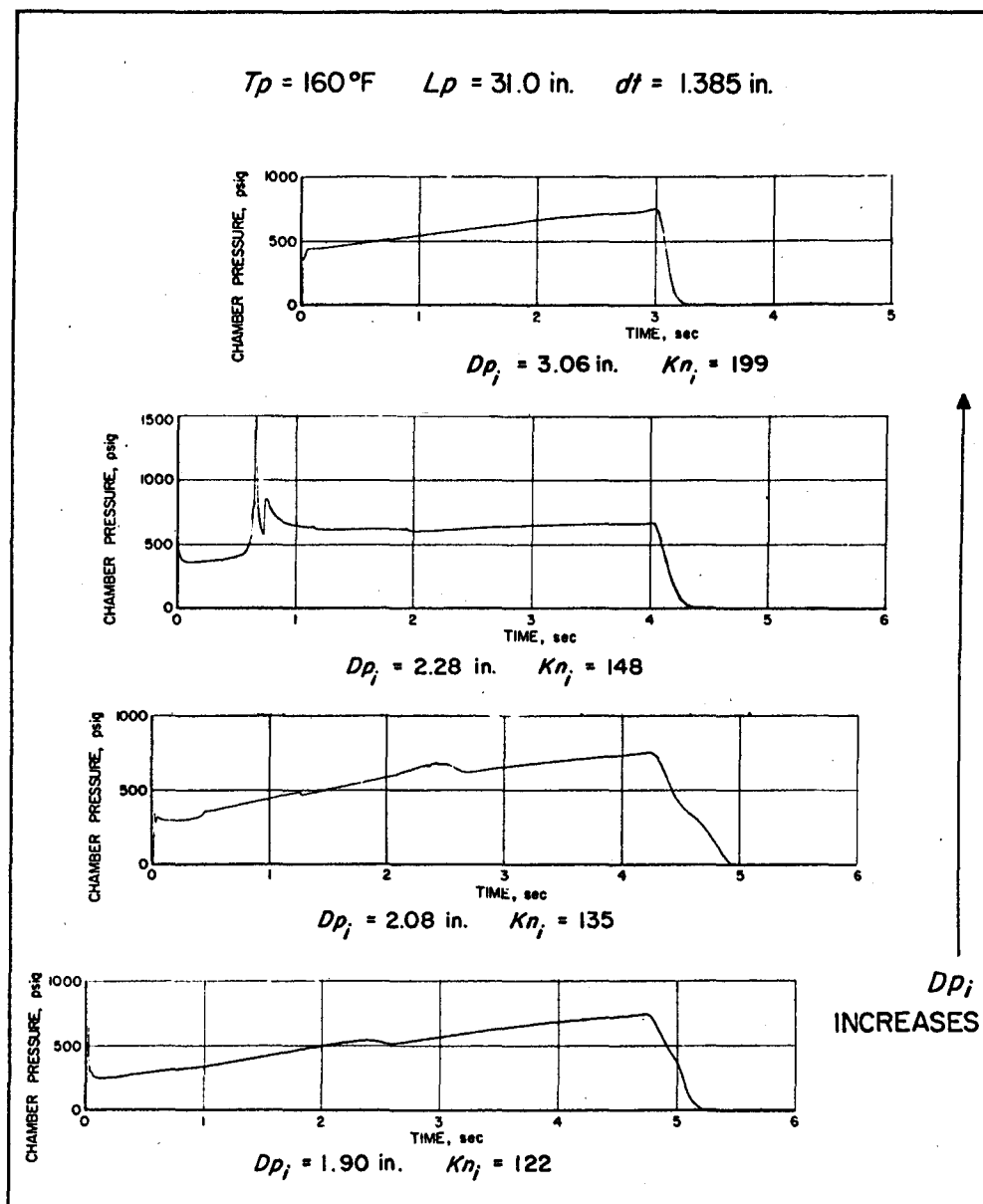


Figure 9. Effect of Varying Initial Port Diameter with Otherwise Fixed Geometry; Nozzle Throat Diameter = 1.385 in.

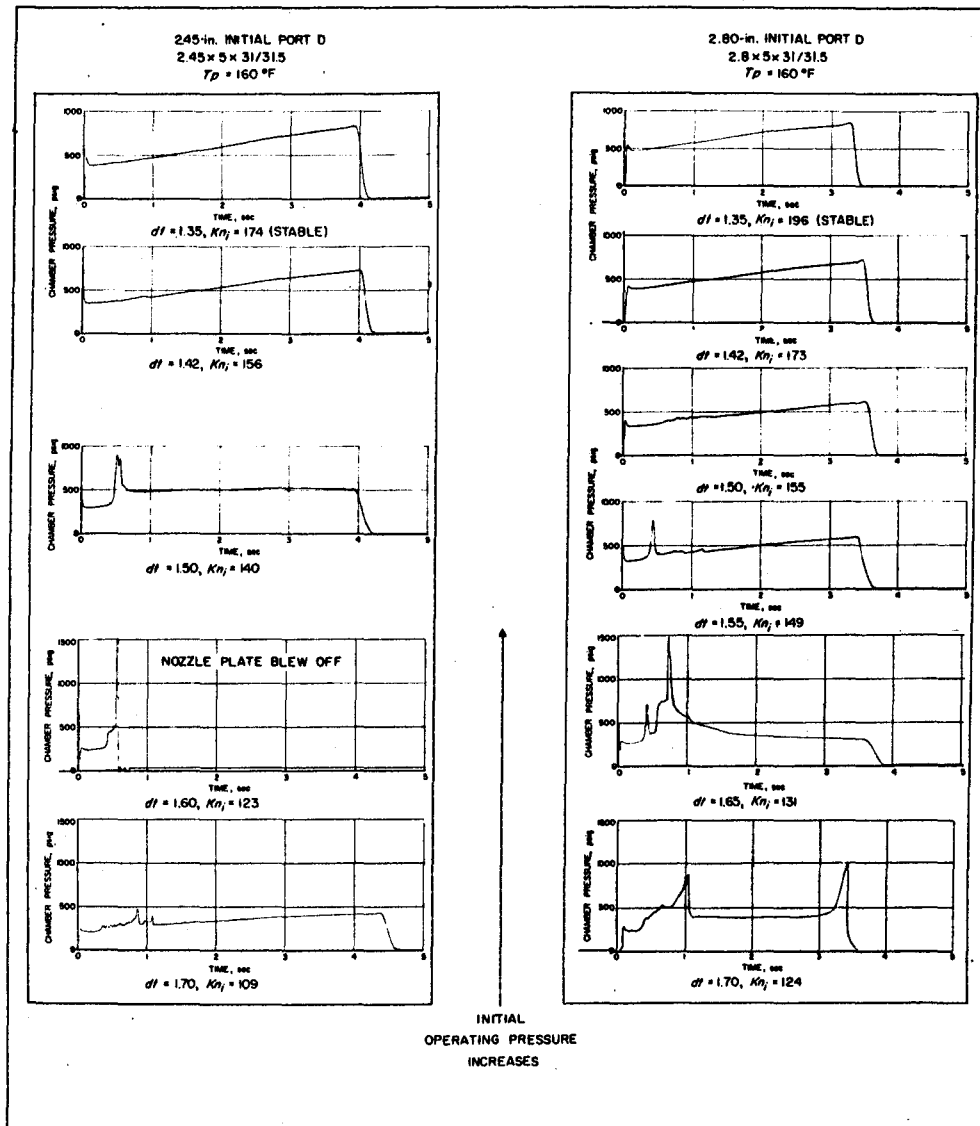


Figure 10. Effect of Varying Operating Pressure Level; 2.45 and 2.80 in. Initial Port Diameter.

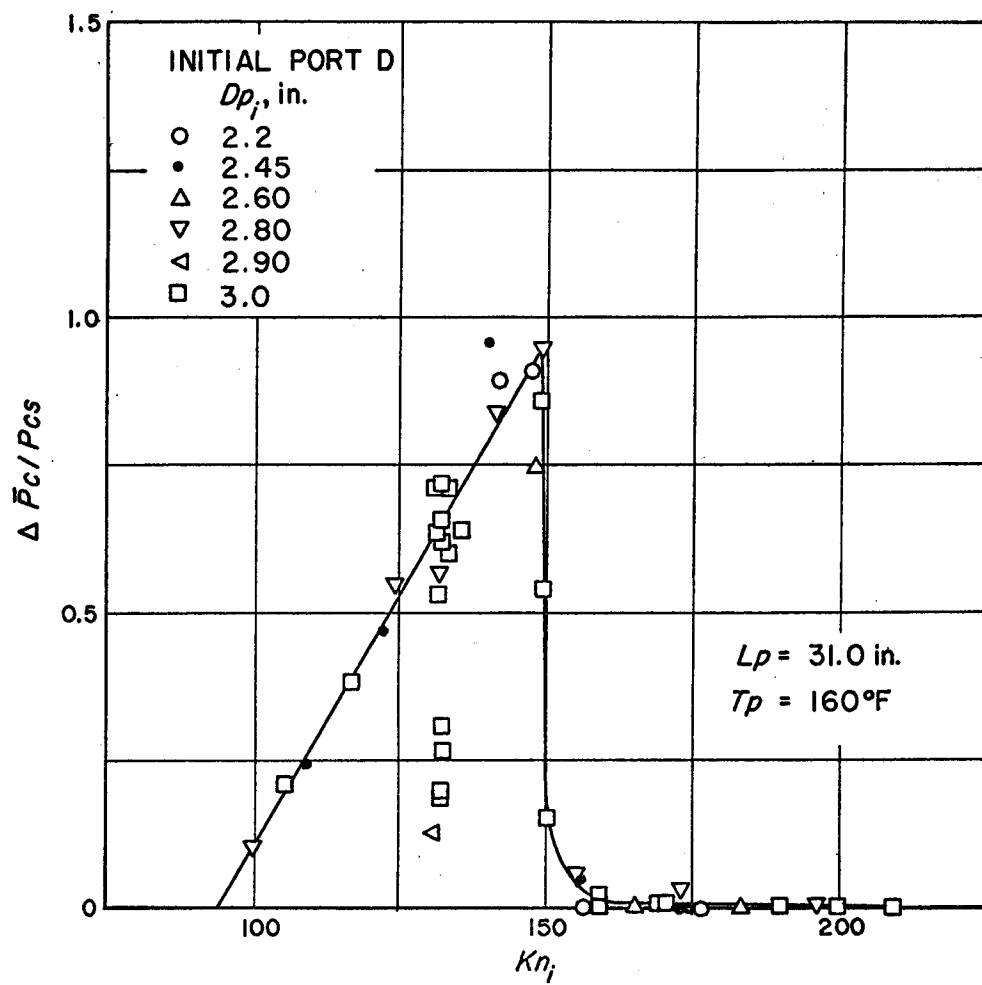


Figure 11. Unstable Increment in Chamber Pressure Versus Initial Value of Area Ratio Kn_i ; Initial Port Diameter 2.2 to 3.0 in. Grain Length 31 in.

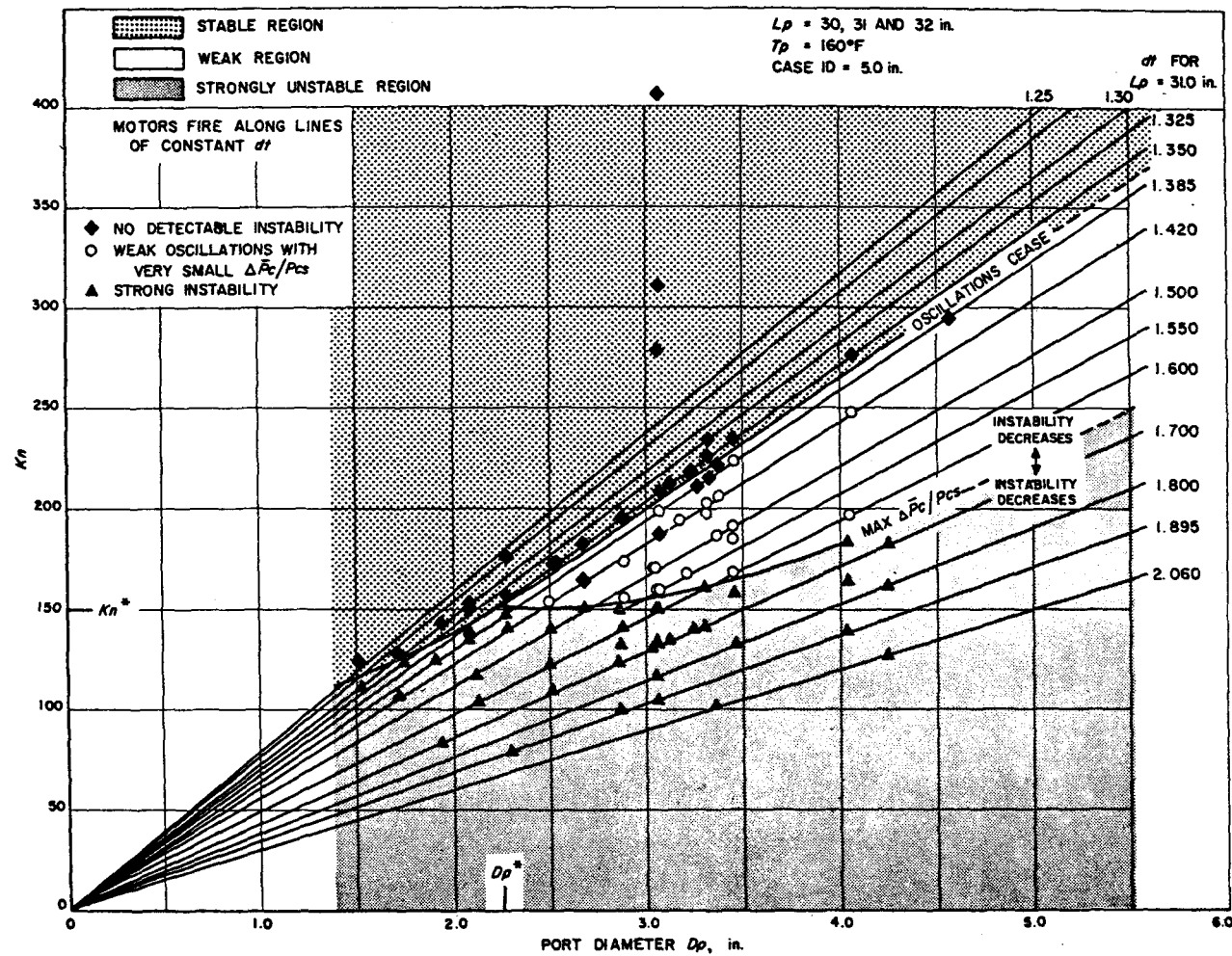


Figure 12 Instability Regions in The Area Ratio Kn , Port Diameter D_p , Plane; Grain Lengths 30, 31 and 32 in.

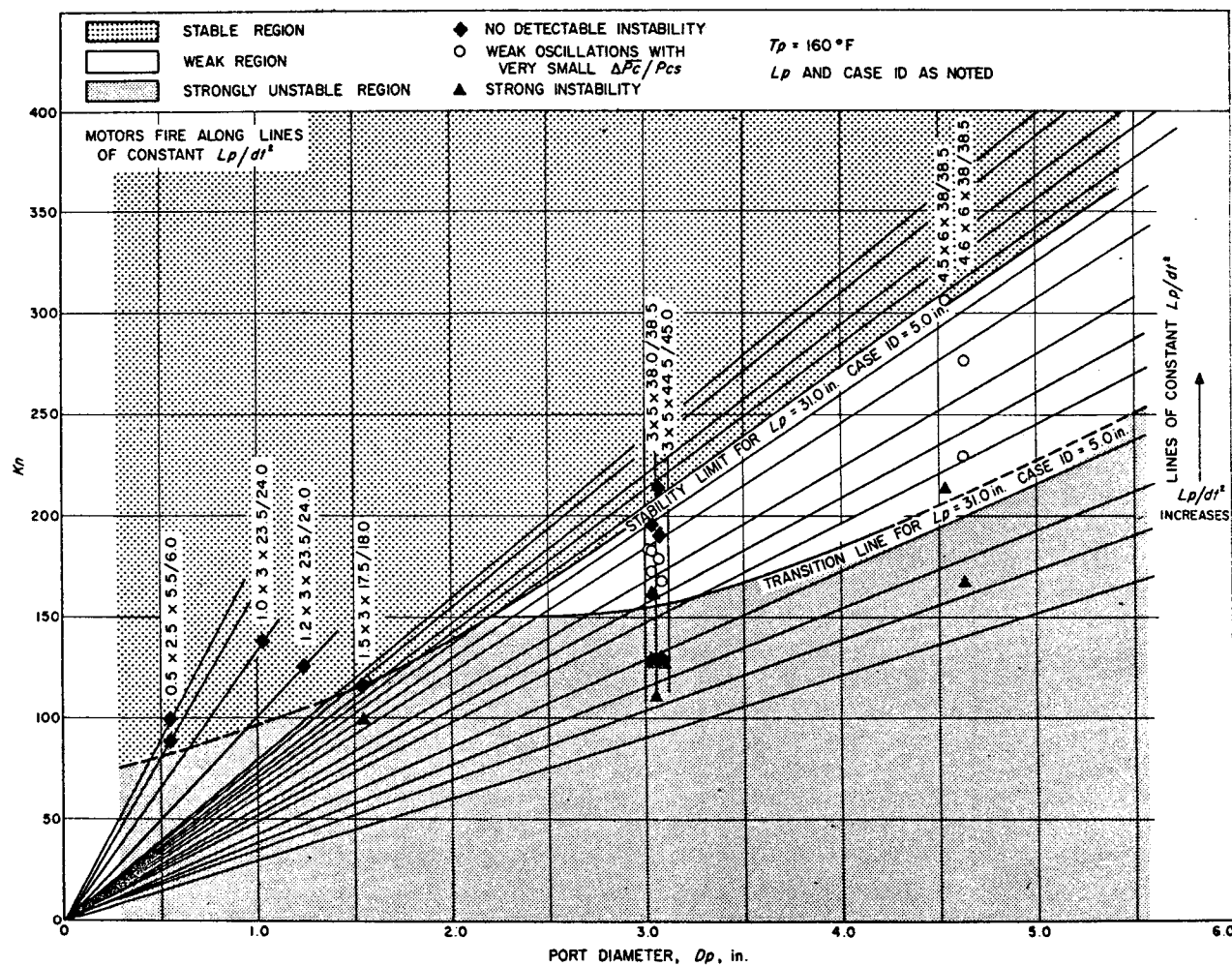


Figure 13. Instability Regions in The Area Ratio K_n , Port Diameter D_p , Plane; Odd Sized Motors.

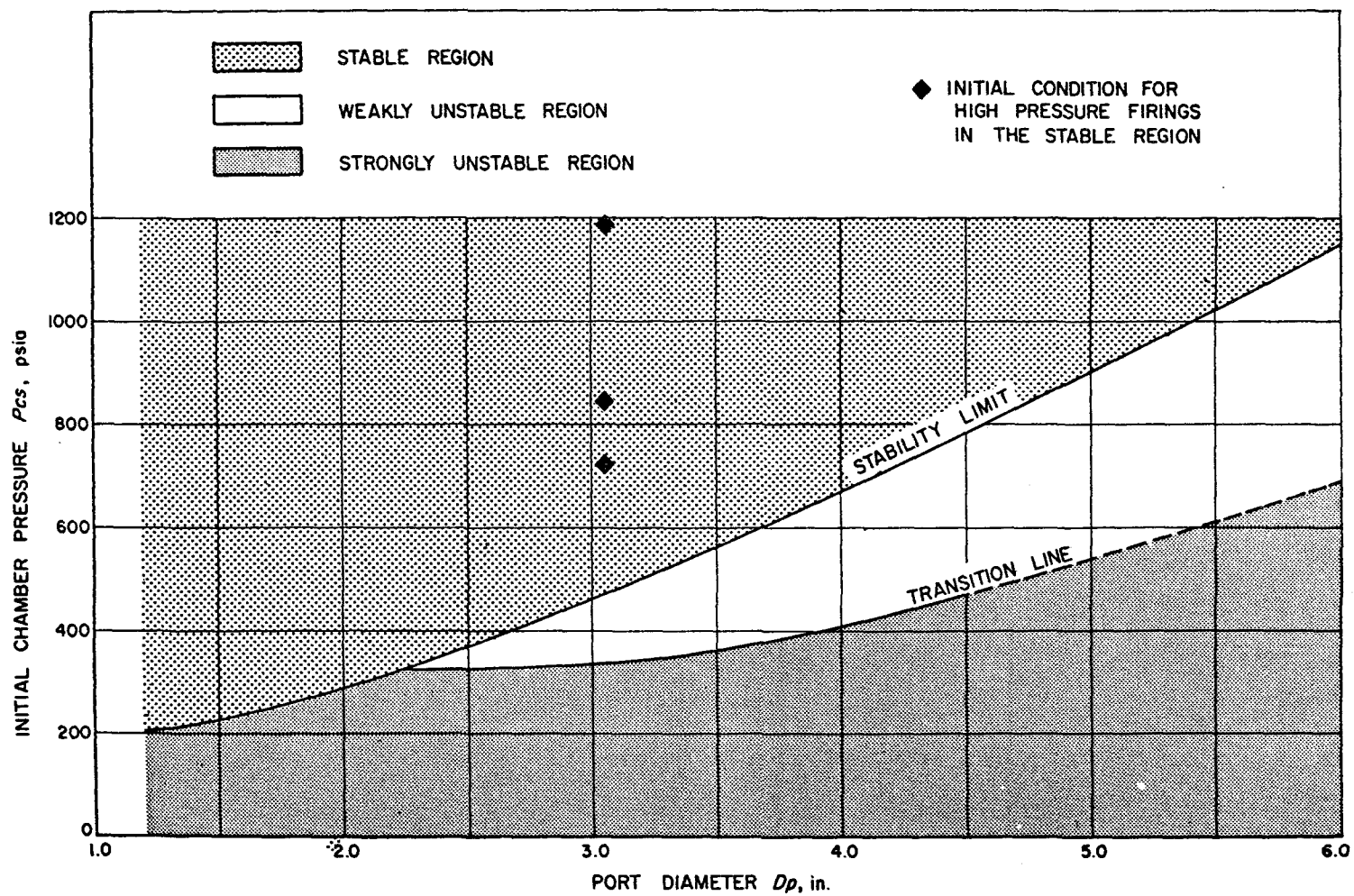


Figure 14. Instability Regions in The Chamber Pressure P_{cs} , Port Diameter D_p , Plane.

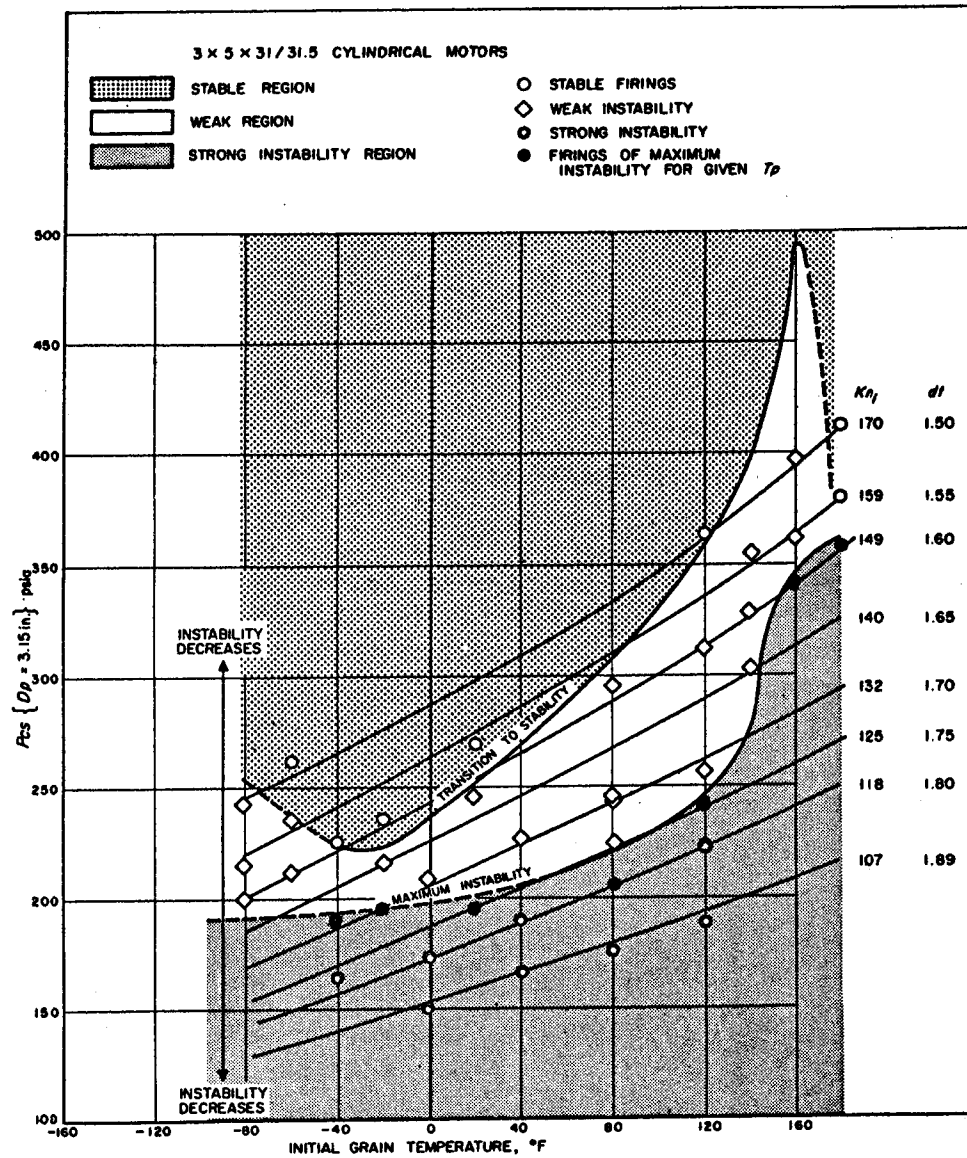


Figure 15. Instability Regions in the Initial Chamber Pressure, Initial Grain Temperature Plane.

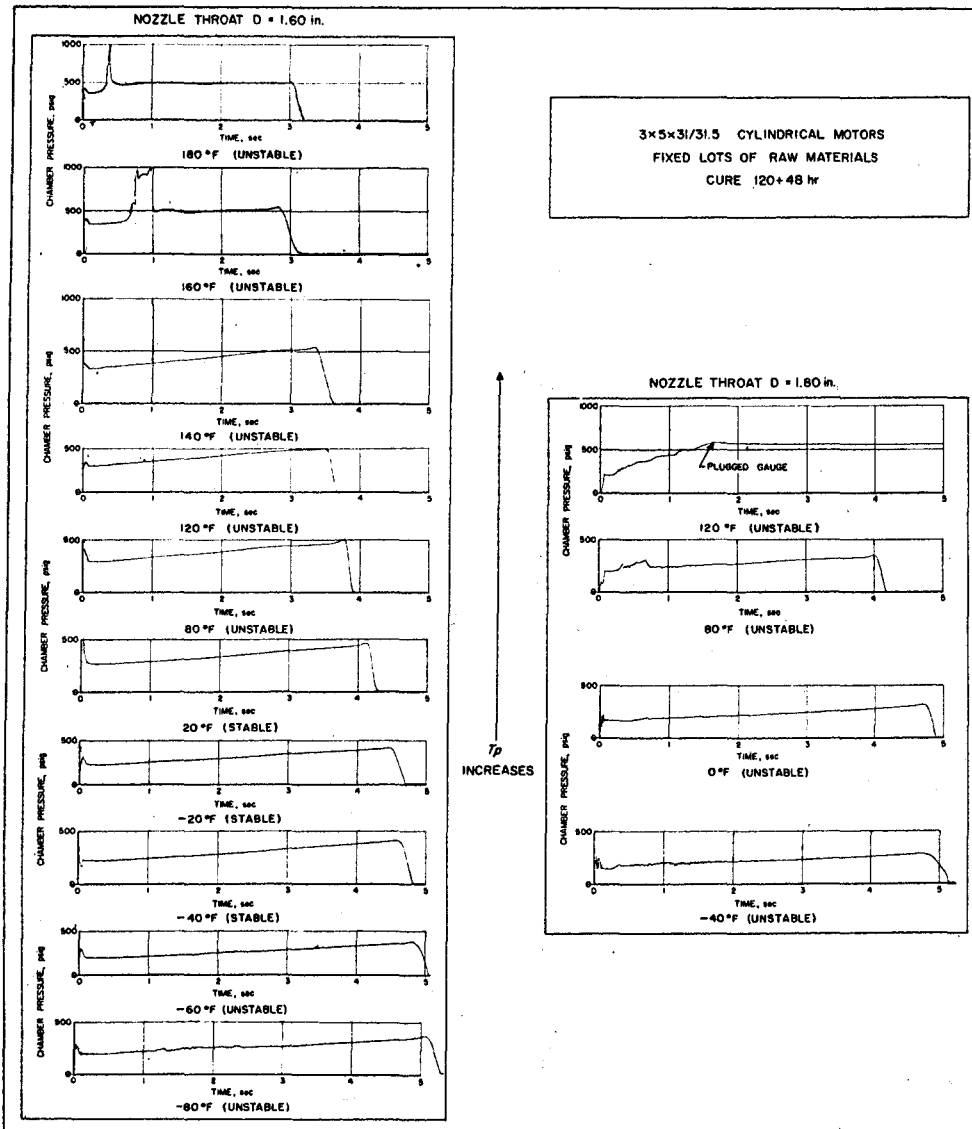


Figure 16. Effect of Varying Grain Temperature With Fixed Geometry;
Nozzle Throat Diameter = 1.60 and 1.80 in.

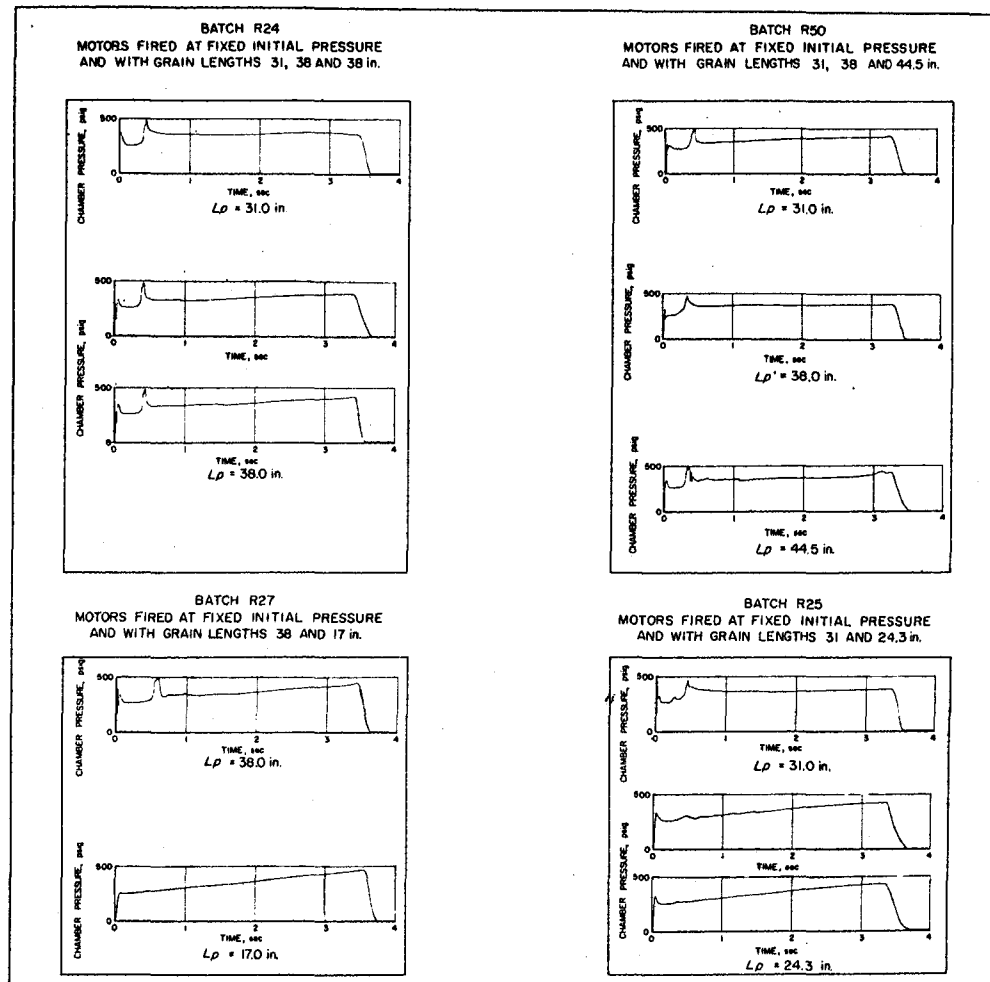


Figure 17. Effect of Grain Length; Mean Chamber Pressure Versus Time Histories of Typical Firings.

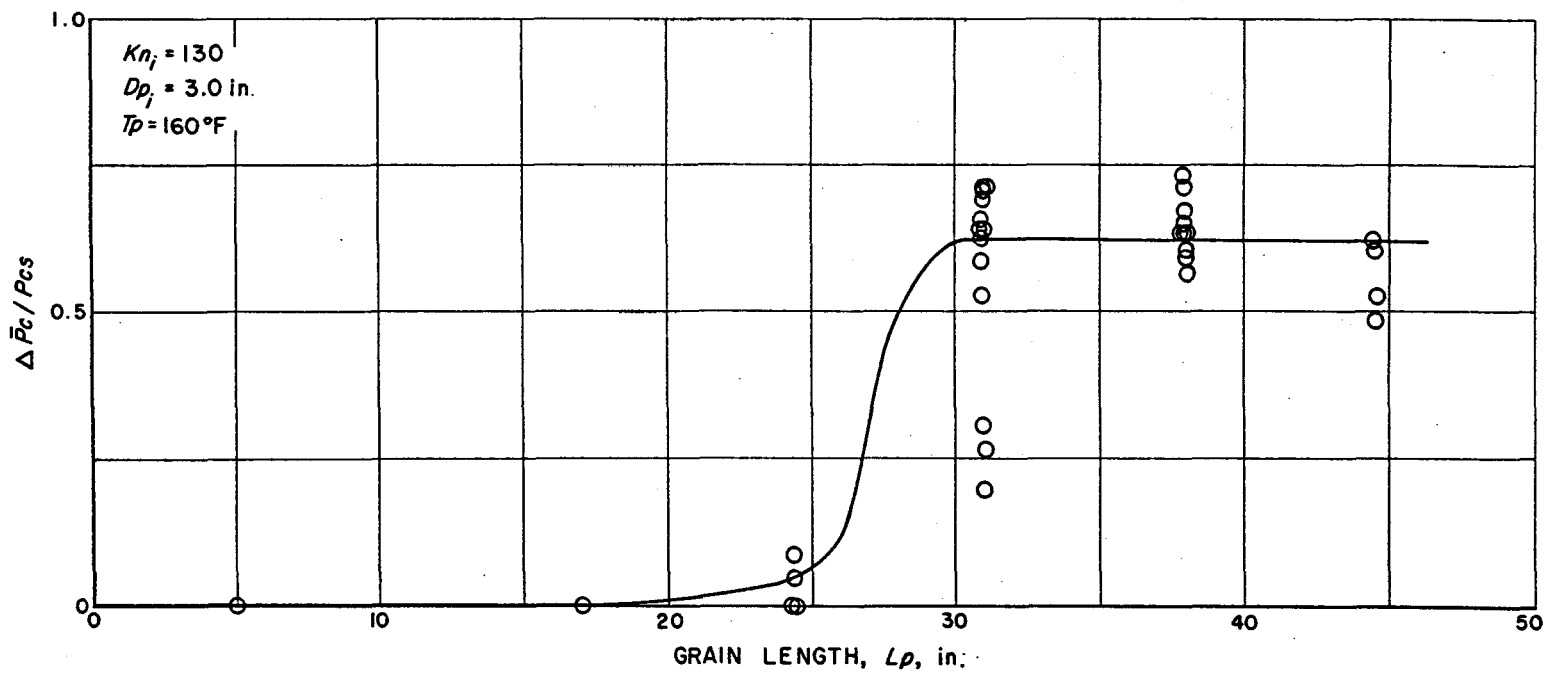


Figure 18. Unstable Increment in Chamber Pressure Versus Grain Length;
Area Ratio $Kn \approx 130$.

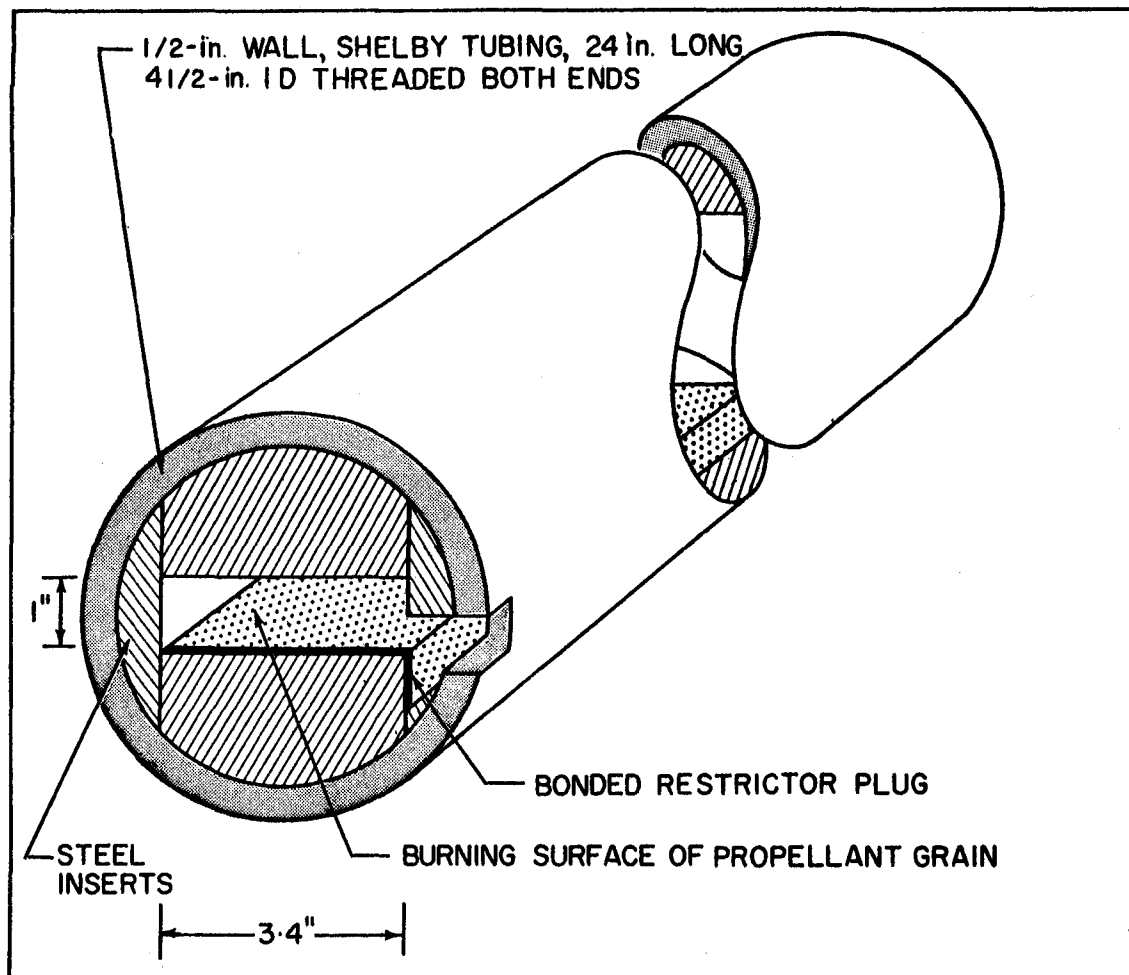


Figure 19. Type 1 Opposed Plane (Slab) Motor Configuration.

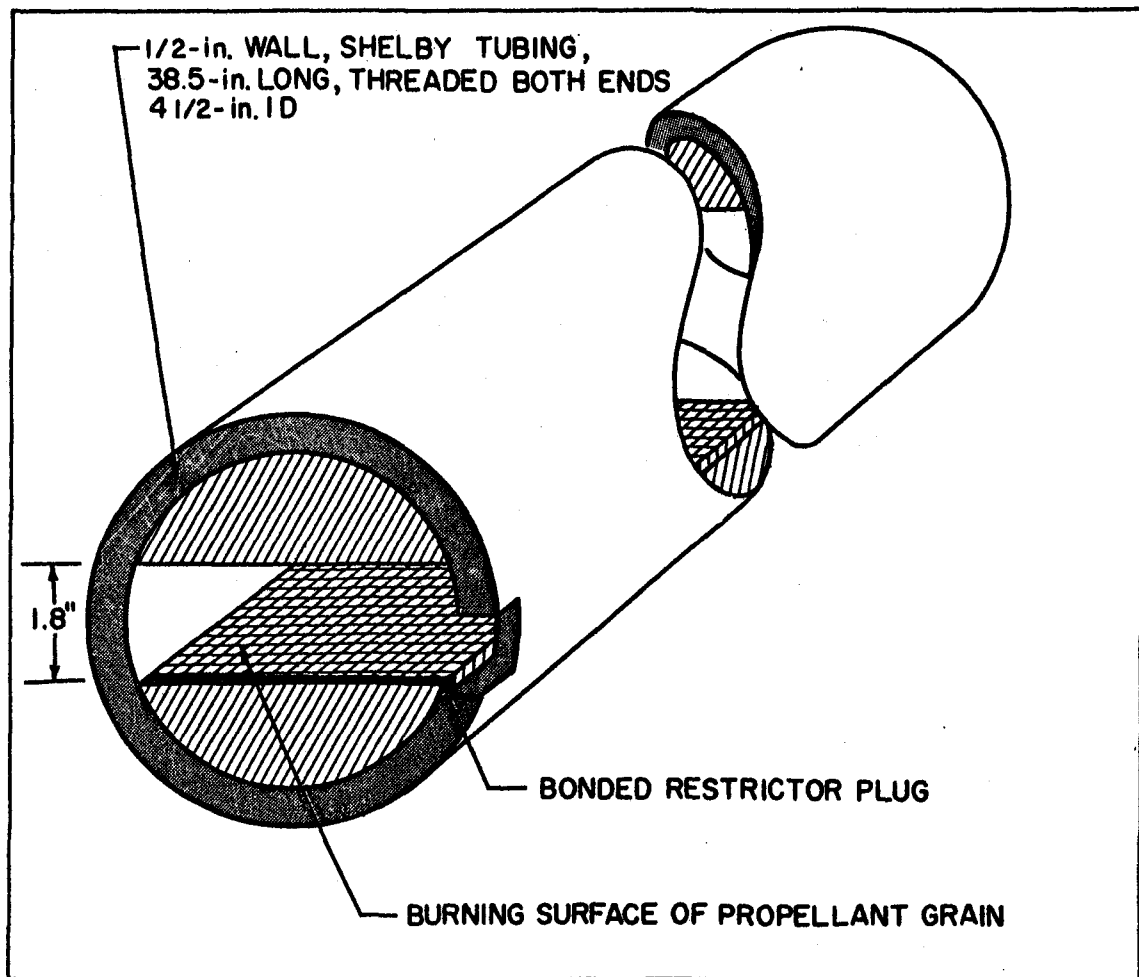


Figure 20. Type 2 Opposed Plane (Slab) Motor Configuration.

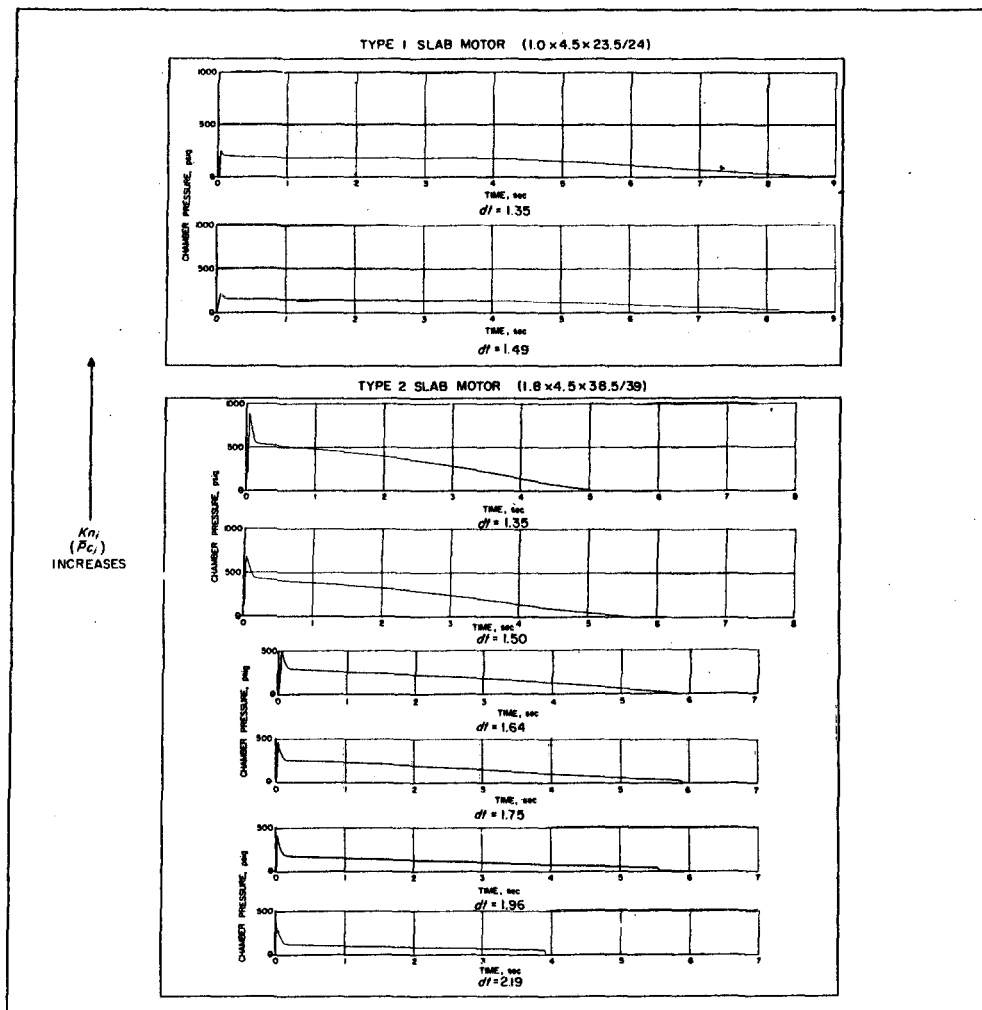


Figure 21. Mean Chamber Pressure Versus Time Histories of Type 1 and Type 2 Slab Motors.